



Calhoun: The NPS Institutional Archive
DSpace Repository

Theses and Dissertations

1. Thesis and Dissertation Collection, all items

1955

The design of a wind tunnel for fuel spray vaporization studies.

Farnsworth, William D.

University of Minnesota

<http://hdl.handle.net/10945/14050>

Downloaded from NPS Archive: Calhoun



Calhoun is the Naval Postgraduate School's public access digital repository for research materials and institutional publications created by the NPS community. Calhoun is named for Professor of Mathematics Guy K. Calhoun, NPS's first appointed -- and published -- scholarly author.

Dudley Knox Library / Naval Postgraduate School
411 Dyer Road / 1 University Circle
Monterey, California USA 93943

<http://www.nps.edu/library>

THE DESIGN OF A WIND TUNNEL FOR FUEL SPRAY
VAPORIZATION STUDIES

A Thesis Submitted to the
Faculty of the Graduate School of the
University of Minnesota

By

William D. Farnsworth
Lt., U. S. Navy

In Partial Fulfillment of the Requirements
for the Degree of
Master of Science in Aeronautical Engineering

August, 1955

Thesis

F 229

ACKNOWLEDGEMENTS

The author wishes to express his sincere appreciation and indebtedness to the following persons who through their considerate assistance made the completion of this paper possible:

To Professor Thomas E. Murphy and Professor M. M. El-Wakil for their technical advice and encouragement.

To Lt. John B. Bailey, U.S.N. and William Alden for their suggestions and physical aid in construction of the apparatus.

To the U. S. Naval Postgraduate School, Monterey, California, which sponsored the attendance of the author at the University of Minnesota as a candidate for the degree of Master of Science.

TABLE OF CONTENTS

	Page
Summary	1
Introduction	3
Wind Tunnel System	5
Design of Wind Tunnel Components	7
The Heater Section	7
The Settling Chamber	8
The Contraction Nozzle	10
The Test Section	11
The Diffuser Section	13
Material of Construction	14
Power System	15
Fuel System	17
Instrumentation	19
Static Pressure	20
Static Temperature	21
Velocity	26
Wind Tunnel Calibration	27
Results and Discussion	29
Conclusions and Recommendations	31
References	33
Appendix	34
List of Symbols	35
Sample Calculations	37

LIST OF ILLUSTRATIONS

Figure

1. Schematic of the Equipment, Suction Pump Configuration	43
2. Schematic of the Equipment, Compressor Configuration .	44
3. Diagram of Wind Tunnel, Side View	45
4. Diagram of Wind Tunnel, Top View	46

LIST OF ILLUSTRATIONS (Cont.)

Figure	Page
5. Photograph of Wind Tunnel and Accessories	47
6. Photograph of the Heater Section Assembly	47
7. Wattage Curves	48
8. Photograph of the Heater Installion	49
9. Photograph of the Settling Chamber and Contraction Nozzle	49
10. Schematic of the Heater Electrical Circuit	50
11. Schematic of the Thermocouple Circuit	50
12. Photograph of the Test Section	51
13. Photograph of the Test Section, Top View	51
14. Curve for Power Plant Displacement	52
15. Wet-Mixture Thermocouple and Stuffing Box	53
16. Photograph of the Test Section, Side View	54
17. Photograph of the Diffuser and Surge Tank	54
18. Photograph of the Suction Pump, Side View	55
19. Photograph of the Suction Pump, Top View	55
20. Photograph of the Compressor and Engine	56
21. Photograph of the Control Panel	56
22. Schematic of the Fuel System	57
23. Calibration Curve of Rotometer for Benzol	58
24. Schematic of the Pressure Measuring System	59
25. Photograph of the Instrument Panel	60
26. Photograph of the Wet-Mixture Thermocouple Probe . . .	60
27. Schematic of Smoke Probe and Test Section	61
28. Velocity Profile, Station 10, Left Tap	62

LIST OF ILLUSTRATIONS (Cont.)

Figure	Page
29. Velocity Profile, Station 10, Right Tap	62
30. Velocity Profile, Station 10, Center Line Tap . . .	63
31. Velocity Profile, Station 18, Center Line Tap . . .	63
32. Velocity Profile, Station 18, Left Tap	64
33. Velocity Profile, Station 18, Right Tap	64
34. Curve to Compute Wet-Mixture Thermocouple Error . .	65

LIST OF TABLES

Number		Page
I.	Velocity Profile Data, Station 10	41
II.	Velocity Profile Data, Station 18	42

SUMMARY

This report discusses the design and construction of a wind tunnel designed primarily to investigate experimentally fuel atomization and vaporization in an air stream. The wind tunnel consists of the normal wind tunnel components, such as settling tank, contraction nozzle, test section and diffuser, plus the addition of a heater section to heat the air passing through the tunnel and a fuel system to inject fuel into the test section. The design of each of these components is discussed in detail.

In using the continuity, momentum, and energy equations when analyzing fuel vaporization, the most helpful parameters are the static pressure, static temperature and velocity. The necessary instrumentation and their design and possible errors are reviewed in detail.

A general outline and discussion of the fuel system and air supply is included.

Structurally the tunnel is fabricated to operate with a partial vacuum of one-half of an atmosphere, since the proposed power system, prior to the completion of the tunnel, was a vacuum pump. The efficiency of the vacuum pump was not high enough; therefore, a power plant driving a compressor furnishes the energy to push the air through the tunnel.

The survey of the flow in the test section is described and the results are discussed.

The project was conducted under the auspices of the Mechanical and Aeronautical Engineering Departments of the University of Minnesota in partial fulfillment of the requirements for the degree of Master of Science.

INTRODUCTION

The design of jet engines for high performance aircraft requires accurate knowledge of the phases through which the fuel-air mixture passes before a combustible mixture is obtained in the combustion chamber. After the fuel leaves the spray nozzle it requires time to atomize and vaporize in the process of forming a combustible mixture. If this time could be reduced this would reduce ignition lag and permit the use of shorter combustion chambers or inner liners in jet engines.

According to El-Wakil (Reference 1), liquid fuel injected into the preignition zone of a combustion chamber leaves the nozzle as a ligament or sheet, then breaks up into a cloud of droplets which are accelerated or decelerated to the air stream velocity by aerodynamic drag forces. During this time the droplets are heating up (or possibly cooling down) to their equilibrium temperature equal to the wet-bulb temperature corresponding to the conditions existing at that moment. Vaporization during this period occurs at a rate determined by (1) the air stream velocity, temperature, and static pressure, (2) the droplet velocity, initial temperature, and diameter, and (3) the physical properties of the fuel used. Thus, by obtaining a survey of the static temperature, static pressure, and velocity of the mixture in the preignition zone of a combustion chamber, and by making certain necessary simplifying assumptions, the vaporization rate of sprays may be calculated.

The method of calculation suggested by this report is the use of the continuity, momentum, and energy equations. The four unknowns in the equations are velocity, static pressure, static temperature, and heat flow. If a value of any one of the unknowns can be determined experimentally, a solution of the equations is possible. Therefore, the wind tunnel presents an excellent opportunity to study fuel sprays.

The wind tunnel discussed in this report is designed with a fuel nozzle located at the entrance of the test section. Thus, the preignition zone of a combustion chamber is simulated by injecting fuel into the test section. This simulation presents the opportunity to measure the changes in the static pressure, the static temperature, and the velocity due to the vaporization of the fuel. As mentioned above, any one of these measured parameters allows the solution of the equations. Once the heat extracted from the air is known, it is possible to correlate this information with the single droplet analysis by El-Wakil (Reference 1), to determine the rate of vaporization.

Wind tunnel testing is a means to an end, and not an end in itself. If tests made in a wind tunnel cause us to think, then that is sufficient justification for having built the tunnel.

WIND TUNNEL SYSTEM

The general overall air flow system consists of a power plant, manifold or ducting, control valves, an air flow meter, and the wind tunnel. A schematic of the system with a vacuum pump as the power source is shown in Figure 1. A schematic of the system with an engine driven compressor as the power source is shown in Figure 2.

The basic wind tunnel is an open circuit type and is symmetrical about the horizontal and vertical axes and symmetrical about its longitudinal axis, except the heater section. The portion of the wind tunnel which is symmetrical about the longitudinal axis has a square cross-sectional area, and the heater section has a rectangular cross-sectional area, (See Figures 3, 4, and 5)

The two control valves, one located downstream of the test section and the other upstream, as shown in Figure 1, were provided to offer a means of having independent control of the velocity and the static pressure in the test section while operating with a vacuum pump. When the power source was changed to a compressor, the valve control, located downstream of the test section, was moved to a position upstream of the air flow meter, as shown in Figure 2. This valve controls the velocity in the test section by bleeding the necessary compressed air into the atmosphere. The vacuum pump was replaced by the engine driven compressor because the pump could not produce the desired velocities. The original valve upstream of the test section became superfluous, but time did not permit the removal of this valve or the construction of another

downstream of the test section to control the static pressure in the working section by controlling the back pressure.

The air flow meter was placed in the ducting, upstream of the tunnel, to supply a means of measuring the rate of mass flow through the tunnel.

All of the wind tunnel dimensions are shown in Figures 3 and 4 and are not listed in the following discussion of the tunnel components.

DESIGN OF WIND TUNNEL COMPONENTS

The design of the wind tunnel components is discussed in the order that these components are encountered by the air stream.

The Heater Section. This section has a rectangular cross-sectional area; therefore, a double entry was provided for the air flow, to obtain a good distribution of the air over the heaters. The rectangular shape, shown in Figure 6, was determined by the heaters elected to supply the heat.

The size and type of heaters installed (230 volt, 2450 watt, Chromolox electric finstrip) were determined by (1) the necessary wattage, (2) the air velocity required past the heaters, and (3) the cost per unit heater, with the latter being the most important consideration.

The wattage required to raise the temperature of the air from 70 F to 500 F is 25,000 watts, when the velocity is 50 feet per second in a test section having a cross-sectional area of 16 square inches. At least 12 of the above heaters are required. This can be seen by the graph in Figure 7. An example of the calculations necessary to construct this graph is shown in example 1 of the Sample Calculations of the Appendix.

The heater watt density required a minimum air velocity of 2 feet per second past the heaters to prevent them from overheating and burning out. In order to keep the cross-sectional area small enough to obtain the necessary velocity, the heaters had to be installed in columns of three. (See Figures 3 and 8)

Budgetary limitations dictated a preliminary installation of only six heaters, although the section was designed and constructed to hold twelve heaters. The heaters are assumed to be 95 per cent efficient; therefore, the six heaters should provide air temperatures up to 250 F with a 50 feet per second air flow in the test section, also shown in Figure 7.

A preheat jacket was built around the heater section, as shown in Figures 3 and 4. The colder air stream flows through this preheat jacket and is heated slightly before it passes through the heaters. This jacket also serves the purpose of insulating the heater section and prevents the loss of heat through the walls.

As mentioned before the heater section was designed so that twelve heaters could be installed in four rows of three. The rows were staggered vertically in order to expose the air to as much heating surface as possible, and to facilitate the mounting of the heaters. Each heater was controlled by an OFF-ON switch. This arrangement made it possible to operate with different air temperatures. With the OFF-ON switch of one of the heaters replaced by a variable voltage transformer, a smooth control of the air temperature throughout the possible temperature range was provided. A diagram of the electrical circuit for the six heaters is shown in Figure 10.

The Settling Chamber. A combination expansion and contraction section was needed to connect the settling chamber to the heater section. (See Figure 6)

The air flow entering the settling chamber will undoubtedly contain a nonuniform distribution of velocity, since it passes

through the compressor, the ducting, a control valve, the air flow meter, the preheat jacket, and the heaters before arriving at the settling chamber. This turbulence is reduced by reducing the velocity in the large cross-sectional area of this chamber and the three damping screens that completely span the settling chamber near the entrance, as shown in Figures 3 and 4.

Schubauer (Reference 2), states that the effectiveness of one screen in damping the oncoming turbulence is well approximated by the formula,

$$f = \frac{1}{\sqrt{1 + k}}$$

or in the case of n screens Reference 3,

$$f = \frac{1}{(1 + k)^{n/2}}$$

where f is the reduction factor and k is the pressure-drop coefficient for the screen. It is obviously more efficient to obtain a desired reduction factor by the use of several screens with small pressure-loss coefficients rather than by the use of a single dense screen. Since the air velocity is low in a large settling chamber, the installation of several damping screens is permissible without excessive penalty for the power absorption or large pressure drops across the screens.

Three 50-mesh screens with wire diameters of .0065 inches were installed in the settling chamber. Schubauer (Reference 2), states that the critical velocity of a 50-mesh screen with a wire diameter of .0055 inches is 15.5 feet per second. Above the critical velocity the eddies shed by the screen were abnormal. Below the critical

velocity the eddies shed fell off rapidly and smoothly. The velocity in the settling chamber was approximately 2 feet per second when a velocity of 50 feet per second was produced in the test section.

The screens action was to break up the larger disturbances into small eddies, which due to viscosity further reduced in size as the flow continued down the settling chamber.

According to Robinson (Reference 4), it is recommended that the length of the settling chamber be at least one and one-half times its effective diameter, in order to allow the flow to become more uniform.

The Contraction Nozzle. A large contraction or area ratio between the settling chamber and test section had several advantages. A large contraction ratio resulted in a low air speed in the settling chamber, thus, permitting the installation of a number of damping screens (as related above) also permitting greater decay of turbulence in a given length of settling chamber. Furthermore, unless the contraction has the effect of greatly increasing the turbulence energy of the stream, the ratio of the turbulent intensity to the mean speed will decrease through the contraction nozzle as the mean speed increases.

Hilton (Reference 5), states that contraction ratios normally employed range from 5:1 to 20:1 approximately. Very low turbulence wind tunnels have been constructed with contraction ratios of as much as 34:1. The contraction ratio of this wind tunnel is 25:1. (See Figures 3, 4, and 9)

The contraction nozzle cross-sectional shape was determined by the cross-sectional shape of the test section and settling chamber, which are square.

The curvature of the contraction nozzles was one-quarter of a second order ellipse with a minor axis of 16 inches and a major axis of 24 inches, except the last inch and one-half leading into the test section, which was straight. The major axis was parallel to the longitudinal axis of the tunnel. Therefore, the nozzle was faired rapidly at first and then very gradually as the test section was neared. The curvature of the nozzle was selected to give a continuously accelerating flow along the axis of the contraction and a continuously decreasing pressure. Hence, there was no danger of boundary layer separation.

The Test Section. The square test section was decided upon because of the desire to mount glass along the entire length of the section on both sides (Figure 12) permitting visual observation of the spray and the use of photographic methods. These requirements were more important than the disadvantage of the thick boundary layers in the corners of a square test section. Also, the ease of manufacture was a deciding factor.

According to Pope (Reference 6), the walls of a closed jet test section should be slightly divergent to counteract the effective contraction due to boundary layer growth, but this was not done due to the complications involved in manufacturing. This fact and the fact that thick boundary layers exist in the corners should be taken into consideration by anyone using this tunnel, by confining

the working area to an area slightly smaller than the cross-sectional area of the test section.

The cross-sectional area of the test section was determined by the velocity desired (50 feet per second) and the displacement of the proposed suction pump to draw the air through the tunnel. The results of the calculations for several test section sizes are shown by the graph in Figure 14. An example of the calculations is shown in example 2 of the Sample Calculations in the Appendix.

The static pressure holes were located in the top wall of the test section along the longitudinal axis. (See Figure 13) The taps through which the velocity and temperature probes were inserted were also located in the top wall of the test section and can be seen in Figure 13, except one that was located in the bottom wall. Two taps were located near the entrance of the test section, but were offset from the center line (one on each side) enough to keep the probes clear of the spray and/or the turbulence produced by the spray nozzle. Three taps were located in the cross-sectional plane 10 $\frac{3}{4}$ inches from the entrance of the test section, one on the center line and the other two, one-inch from the center line, one on each side. In the cross-sectional plane, 18 $\frac{3}{4}$ inches from the entrance are four taps, three located in the top wall with the same arrangement as the three in the 10 $\frac{3}{4}$ inch plane, but the fourth tap in the bottom wall on the center line.

Since two total pressure probes and three temperature probes were fabricated, five stuffing boxes, designed to fit around the probes, were constructed that would screw into the above discussed taps. (See Figure 15) Plugs were machined to close the unused

taps and were interchangeable with the stuffing boxes. Thus, the instruments or probes could be moved around from tap to tap as desired.

The glass walls of the test section were one-half inch thick, consisting of one-quarter inch plate glass on the inside and one-quarter inch safety glass on the outside. If higher temperatures than the 250 F expected from the six installed heaters are desired, it is recommended that these glass walls be replaced by pyrex or other transparent material that can withstand high temperatures.

A picture of the test section with the glass walls and the instruments installed is shown in Figure 16.

The Diffuser Section. The diffuser section was a combination diffuser and surge tank, as can be seen in Figures 3, 4 and 17.

The function of the diffuser is to turn the kinetic energy of the air in the working section back into pressure energy, with a minimum of loss. It is the diffuser that determines the mechanical efficiency of the tunnel almost entirely. A large area-expansion ratio is essential for high efficiency. Since the rate of expansion is limited to approximately 8 degrees between opposite walls (References 4, 5, and 6), the area-expansion ratio of the diffuser was limited to 7:1, due to the size of the room in which the tunnel was operated.

The diffuser was manufactured with a square cross-sectional shape, an expansion rate of 8.3 degrees between walls, and a 50-mesh screen covering the outlet. This screen was placed there to assist the two screens in the surge tank in damping out any surges from the suction pump.

The diffuser was located inside a tank which serves the purpose of a surge tank. The expansion rate of this tank was 20 degrees between opposite walls until it reached a cross-sectional area of 400 square inches, the cross-sectional area then remaining constant to the end of the tunnel. In this constant area portion of the surge tank two 50-mesh screens were installed, completely spanning the tank. These screens and the additional volume were to serve the sole purpose of damping out surges from a suction pump. Four spring loaded safety valves were designed and incorporated into the walls of the constant area portion of the surge tank, one on each side. (See Figures 3 and 4) The flow through the diffuser section is a mixture of air and fuel vapor; therefore, the safety valves are necessary in case this mixture is accidentally ignited and the inevitable explosion follows.

Material of Construction. Since this wind tunnel was designed primarily to operate under partial vacuums up to one-half of an atmosphere, one-eighth inch hot rolled carbon steel, reinforced by belts of channel and angle iron, was used, except in the test section. The top and bottom walls of the test section were fabricated out of one-quarter inch cold rolled carbon steel, and glass was installed for the two side walls, but reinforced by frames of one-eighth inch hot rolled carbon steel. A belt of angle iron around each end of every section served the purpose of flanges, by which each section was connected to the other.

POWER SYSTEM

The original proposal for a power plant consisted of a suction pump attached to the tunnel exit to draw the air through the system and produce static pressures in the test section less than the atmospheric pressure. Since no suction pump was available, it was decided to use an old 4 cycle, 4 cylinder, Wright-Gypsy aircraft engine (See Figure 18), as a suction pump. This engine displaced 318 cubic inches, but when operated at 2000 rpm this displacement was not enough to produce the desired velocity of 50 feet per second in a 16 square inch test section. A displacement of 570 cubic inches was required as can be seen in Figure 14. Therefore, the engine was converted to a two-cycle suction pump in order to get the necessary displacement. This conversion was done by removing the original head and replacing it by a head that had reed valves incorporated. The reed valve arrangement was such that four valves, located on one side of a one-half inch aluminum plate, opened, and four other valves, located on the other side of the aluminum plate, closed during the down-stroke of each cylinder, and visa versa on the upstroke. The manifold leading to the valves was divided in half by a baffle, making it possible to isolate the air pulled into the pump from the air exhausted by the pump. (See Figure 19)

It was anticipated that the pump would have a volumetric efficiency of 80 per cent and while operating at 2000 rpm, would produce the desired 50 feet per second air velocity in the test section. But the pump proved to be unsuccessful, for the maximum possible

velocity obtainable was approximately 30 feet per second. Thus, the pump was only about 60 per cent efficient and this was far from satisfactory. The prime mover for the suction pump was an eight-cylinder Hudson automobile engine.

Due to the lack of time no effort was made to secure another suction pump, but the permanent installation located in the turbine test cell of the Mechanical Engineering Department was connected to the tunnel to furnish the power. Photographs of the installation and its control panel are shown in Figures 20 and 21.

This installation consisted of a gasoline powered Lycoming Model O-435-T air-cooled Army tank engine, rated at 162 hp at 2800 rpm driving a centrifugal compressor. The compressor is a 7.48:1 gear ratio supercharger taken from an Allison V-1710 aircraft engine. The speed of the blower is controlled by throttling the engine.

This power system was connected to the upwind end of the wind tunnel. Therefore, the air is blown through the tunnel instead of sucked through, and the desired static pressures below the atmospheric pressure are no longer obtainable.

FUEL SYSTEM

The fuel system consists of a pressure source, a fuel tank, a filter, a rotometer, a water cooling jacket, a fuel nozzle and the necessary pressure gages and shutoff valves. A diagram of the system is shown in Figure 22.

The pressure was furnished by a pressurized carbon dioxide gas tank, which has a pressure reduction valve attached to control the pressure desired in the system.

The fuel tank was a hot water heater cut down in size to hold approximately 5 gallons of fuel, and it had the necessary fittings incorporated. The tank withstood a test of 200 pounds per square inch without any leaks.

A Sperry Gyroscope fuel filter, serial number 644100, was connected to the outlet of the fuel tank.

The house water system was fed into the fuel line downstream of the filter, as shown in Figure 22, in order to be able to check the rest of the fuel system without wasting fuel.

A Schutte and Koerting rotometer, serial number 427178, was incorporated in the fuel system to measure the rate of fuel flow. The rotometer scale was for gasoline, specific gravity 0.71. Since it was anticipated that the fuel used would be benzol, specific gravity 0.87, the rotometer was calibrated, and the calibration is shown in Figure 23.

The rotometer was followed by a shutoff valve and a pressure gage. The pressure gage was limited to 125 pounds per square inch; thus, the fuel system was limited to the same pressure. If higher

pressures are desired this pressure gage must be replaced by a pressure gage that reads higher pressures.

The fuel line, a one-quarter inch flexible copper tubing, entered the settling chamber through a one-half inch water pipe where it was enclosed until it was connected to the spray nozzle. The nozzle was attached to the end of the one-half inch water pipe, which was supported by guy wires at the entrance of the contraction nozzle. The last three inches of the pipe tapered down until the outside diameter at the end was equal to the outside diameter of the nozzle. This arrangement eliminated some of the turbulence behind the spray nozzle.

The cooling system for the fuel line inside of the tunnel consisted of a three thirty-seconds inch flexible copper tubing, which was also located inside of the one-half inch water pipe with the fuel line. This copper tubing carried water up to the end of the pipe, and then the water flowed back down the water pipe, enveloping the fuel line. The water was supplied by the house water system and was connected as shown in Figure 22.

A Monarch fuel nozzle was installed at the end of the water pipe and had a flow rate of five gallons per hour, a spray cone of 30 degrees, and was rated as a high velocity nozzle.

INSTRUMENTATION

The required instrumentation to measure the static pressure, the static temperature and the velocity at different points in the fuel spray is static pressure taps, temperature probes, and total pressure probes.

To facilitate the discussion of the pressure measuring instruments, a description of the manometer system is presented first, and the arrangement is shown in Figure 24. The manometers are located on the instrument panel and a picture of this panel is shown in Figure 25.

The static gage pressure at the entrance of the test section was measured by a mercury manometer, which had one end open to the atmosphere and the other end connected to the static pressure orifice at the upwind end of the test section. The alcohol reservoir for the bank of manometers was subjected to the same static pressure. Therefore, each manometer in the bank of manometers measured a differential pressure which was the difference between the pressure the manometer was to measure, and the static pressure at the entrance of the test section.

The surface area of the alcohol in the reservoir was much larger than the cross-sectional area of the manometer tubes, so that the change of reservoir level could be neglected without incurring too large an error in the manometer board readings. The large reservoir presented the problem of bleeding the pressure into or out of the reservoir fast enough to eliminate delays in the manometer system. Therefore, the reservoir was connected to its

pressure source by a diameter tubing larger than the tubing connecting the rest of the system.

Alcohol was used in the bank of manometers because its low specific gravity is productive of a higher fluid column than is obtained with water. This use of alcohol in place of water allows small changes in pressure to be read more accurately.

An inclined manometer was mounted on the instrument panel with one end connected to a static pressure hole at the upwind end of the test section, and the other end connected to a static pressure hole at the downwind end.

Static Pressure. The detection of a static pressure on a wall, which is a natural boundary of the flowing fluid, is relatively simple since, with properly designed taps, there is no problem of inflow. The requirements for properly designed taps are (1) they should be small in size, (2) drilled perpendicular to the surface, (3) smooth - no burrs permitted, and (4) have symmetrical holes.

The static pressure holes in the test section were .04 inches in diameter, made with the smallest drill available in the machine shop.

The perpendicular requirement was assured to the degree that a power drill was accurate.

The inside wall of the test section was polished to a high gloss to assure the removal of all burrs.

The holes should be perfectly round, or as round as a drill rotating at high rpm could make them.

Therefore, the accuracy of the pressure readings from the static pressure taps should be as accurate as the recording instrument.

Twenty static pressure holes, one inch apart, were drilled in the top of the test section along the center line or longitudinal axis. The static pressure hole at the extreme upwind end of the test section was connected to the reservoir of the bank of manometers and the reservoir of the mercury manometer. The inclined manometer was connected to the third static pressure hole from the upwind end of the test section and to the extreme downwind static pressure hole. The rest of the static pressure taps were connected to the manometers in the bank of manometers as shown in Figure 24.

Therefore, due to fuel vaporization the small changes in static pressure along the test section could be observed in the bank of manometers, and the difference in static pressure at the upwind end of the test section and the downwind end, or total change in static pressure, could be observed on the inclined manometer. The total change in static pressure along the test section was a critical measurement. Thus, the more sensitive inclined manometer was used for this measurement.

Static Temperature. At low velocities, such as the anticipated velocities in the test section, the difference in the stagnation temperature and the static temperature of the air stream is negligible. Thus, no effort was made to try to design a temperature measuring device to measure the exact static temperature, which was the temperature desired.

The simple thermocouple was the temperature sensing element elected to measure the temperatures because (1) it has very little mass - it can be made small enough to fit into the test section without upsetting the flow pattern, and (2) there is practically

no limitation on the distance between the thermocouple and the measuring instrument. The iron-constantan type thermocouple, normally used to measure temperatures from about 0 F to 1400 F, was the type fabricated to measure all temperatures.

The thermocouples to measure the fuel temperature and air temperature at the entrance of the test section presented no problem to construct. But the thermocouple probe, designed and constructed to attempt to measure the fuel vapor-air mixture temperature inside the fuel spray, hereafter called wet-mixture probe, presented the real problem.

The thermocouple to register the temperature of the fuel was simply the junction of the iron-constantan wires placed inside the fuel line at the base of the 200-mesh filter of the fuel nozzle. Naturally, the leads from the junction were insulated from the walls of the fuel line. The tap through which the leads from the thermocouple were inserted was a potential source of trouble or fuel leaks if fuel pressures above 70 pounds per square inch were used. The accuracy of the recording of this thermocouple should be within desired tolerances, for the sensing element is continually bathed in the fuel flowing through the fuel line. It was realized, of course, that the temperature of the fuel will drop a little when it flows through the spray nozzle, but the temperature will have to be assumed the same.

The thermocouple probe to measure the air temperature at the entrance of the test section was constructed with a cylindrical radiation shield around the sensing element. The axis of the cylindrical shield was parallel to the direction of flow; therefore,

the thermocouple was entirely exposed to the air stream. The radiation shield served the purpose of reducing the effect of the wind tunnel walls on the sensing element. The element "sees" the warmer shield bathed in the hot air rather than the colder tunnel walls; thus, little error in the temperature recorded was expected.

The wet-mixture probes required a design that would not let the thermocouple get wet and still let it be exposed to the air-vapor mixture in order to record its temperature. So far this type of temperature probe has never been successfully designed. Two types of wet-mixture probes have been used, one which centrifuges the liquid drops out of the stream and passes the dried gas over the thermocouple, and another which relies on a nonwetting coating on the probe to prevent adhesion of the liquid. Neither type has been developed into a completely reliable probe, according to Mardowski (Reference 7). Therefore, the idea was tried of placing the thermocouple behind a baffle, which would divert the liquid droplets away from the sensing element and allow the eddies behind the baffle to circulate the gases around the element. A schematic and a picture of the design are shown in Figures 15 and 26.

The first baffle is a right circular cone with a 60 degree apex angle, the second and third baffles are a frustum of a right circular cone with an apex angle of 20 degrees, and the fourth baffle is a frustum of a right circular cone with a 10 degree apex angle. The baffles are approximately one-eighth of an inch apart to allow the eddy effect behind each baffle to circulate the air-vapor mixture throughout the probe and around the thermocouple. The baffles were connected together by three piano wires, and the

fourth baffle was attached to the stem of the probe, which was supporting the whole arrangement.

It was anticipated that the first baffle would become entirely wet and would be at the temperature of the liquid. But, since momentum would be imparted to the liquid droplets in a direction away from the axis of the thermocouple probe by the first baffle, the second baffle would be less wet and would reach a temperature determined somewhat by the air-vapor mixture. Therefore, it would be at a temperature closer to the desired temperature. The third baffle would be protected by the first two baffles and should be even closer to the desired temperature. The thermocouple was located in the center of this third baffle. Two of these wet-mixture probes were constructed.

The approximate error that can be expected in the temperature readings from the wet-mixture thermocouples can be determined mathematically, because the heat flow by convection into the thermocouple from the hot air-vapor mixture is equal to the heat flow by radiation out of the thermocouple to the surfaces that it "sees", during steady state conditions.

The heat flow into the thermocouple can be expressed as,

$$\frac{Q}{A} = h(T_a - T_t)$$

where Q is the heat flow, A is the surface area of the sensing element, h is the heat transfer coefficient, T_a is the temperature of the air-vapor mixture and T_t is the temperature the thermocouple is recording.

The heat flow out of the thermocouple mathematically is,

$$\frac{Q}{A} = \sigma \epsilon (T_t^4 - T_b^4)$$

where σ is the well known constant 0.1728×10^{-8} , ϵ is the emissivity or radiation quality of the thermocouple, and T_b is the temperature of the baffle surrounding the thermocouple.

Under steady state conditions,

$$Q_{in} = Q_{out}$$

as stated above, or

$$h(T_a - T_t) = \sigma \epsilon (T_t^4 - T_b^4).$$

A sample calculation to determine the possible percentage of error for a given set of temperature conditions is shown in the Appendix, example 3.

The three thermocouples installed in the test section were supported by hypodermic needle tubing, which could traverse the test section from top to bottom, since they were mounted in the before mentioned stuffing boxes.

All four of the thermocouples were hooked up in parallel to a bus bar with selective switches, and the recording instrument was connected to leads on the bus bar that are common to all other leads, provided the circuit is closed by the proper switch. A Leeds and Northrup direct reading potentiometer, serial number 95979, with a double range of 0-500 F and 0-2000 F and designed for iron-constantan thermocouples, was the instrument connected to the common leads of the bus bar. A schematic of the circuit is shown in Figure 11.

Velocity. The two velocity probes are manufactured out of hypodermic needle tubing, which has an outside diameter of .082 inches and an inside diameter of .060 inches. Robinson (Reference 4), states that the larger the total pressure opening as compared to the tube diameter the more reliable the reading when the instrument is yawed. Therefore, the inside diameter of the probes near the head of the instruments was made as large as possible.

The velocity probes were connected to the two outboard manometer tubes of the bank of manometers, and they were located in the test section so that the forward end of each probe was in the same cross-sectional plane as a static pressure tap. These static pressure taps were also connected to manometers in the bank of manometers. Thus, the dynamic pressure could be read directly from the manometer board in inches of alcohol.

The change in velocity of the air stream, due to the vaporization of the fuel, was one of the essential measurements. Therefore, one of the total head probes was located near the entrance of the test section and the other was near the exit. They were installed so that they could be traversed across the tunnel from top to bottom.

WIND TUNNEL CALIBRATION

The calibration of the cross-sectional velocity variation in the test section is a must in order to use the tunnel intelligently. Ideally, a survey of velocity across the wind tunnel test section should show no change in velocity. Actually, due to imperfect design or construction, there always are small changes.

Before a survey of the velocity in the test section was conducted, the direction of flow was determined fairly accurately by using a smoke probe. The results were very satisfactory for it proved there was very little cross flow. Since the available smoke generator was not designed to operate against pressure and the pressure in the tunnel was above atmospheric, the smoke emanating from the probe was not very dense. Therefore, no effort was made to obtain a photograph of the operation, but a diagram of that which was seen is shown in Figure 27.

The total head probes were then used to obtain a velocity profile, at approximately 100 feet per second in the cross-sectional plane 10 $\frac{3}{4}$ inches from the entrance of the test section, and in the cross-sectional plane 18 $\frac{3}{4}$ inches from the entrance. These planes are hereafter referred to in this report as station 10 and station 18. At each station three surveys were conducted, (1) with the velocity probe located in the center line tap, (2) with the probe located in a tap in the same cross-sectional plane but offset one inch from the center line, and (3) with the probe located in the tap one inch from the center line on the other side. The surveys were done by traversing the probes step by step across the test section from top to bottom.

The alcohol manometers which registered the dynamic pressure picked up by the velocity probes in the test section were the two outboard manometers of the vertical bank of manometers. The possible error in reading these manometers was approximately plus or minus .03 of an inch of alcohol. Also, the power plant did not retain an absolutely constant pressure in the test section. This pressure fluctuation made it more difficult to get an exact reading. Thus, the data obtained were read to the nearest .05 of an inch of alcohol.

RESULTS AND DISCUSSION

Since this report is primarily a descriptive analysis of the design and construction of a wind tunnel, the results were limited to the data and results of the velocity survey in the test section. The data are listed in Table I and II and the calculated results are shown in graph form in Figures 28 through 33. A sample calculation is shown in the Sample Calculations of the Appendix, example 4.

These results proved that the flow at a cross-sectional plane in the test section was at a fairly uniform velocity, except where it was disturbed by the fuel nozzle and the walls.

The graphs in Figures 30 and 31 show the results of the surveys at stations 10 and 18, with the velocity probes located in the center line taps. These velocity profiles definitely indicate that the velocity near the longitudinal axis of the test section is slower than the velocity in the rest of the cross-sectional plane, except near the walls. This slower velocity was anticipated since the fuel spray nozzle was located on the longitudinal axis, and the flow along this axis of the test section was affected by the wake behind the nozzle. This was not considered detrimental to the analysis of a fuel spray in a moving air stream, for a nozzle produces the same effect in an actual combustion chamber.

The remaining four graphs, Figures 28 and 29 for station 10 and Figures 32 and 33 for station 18, are representative of a good turbulent flow profile. Therefore, it could be assumed that the velocity profile was good along the entire length of the test section.

The comparison of the results at station 10 with the results at station 18 revealed the fact that the boundary layer thickness increased between the two stations. This increase should be taken into consideration when experimental data of a fuel spray are being taken, by limiting the survey area to an area within the boundary layers.

CONCLUSIONS AND RECOMMENDATIONS

The results of the test section velocity survey indicated that the design and construction of the wind tunnel were within the allowable limits for research and study of fuel vaporization in a moving air stream.

It is recommended that a few additions and improvements be incorporated into the tunnel such as:

- (1) an addition of six more heaters, since the vaporization of fuel and the diffusion of the vapor are functions of vapor pressure, and the vapor pressure is an exponential function of the temperature
- (2) insulate the tunnel up to the entrance of the test section to limit the escape of heat through the tunnel walls
- (3) the temperature probes should be brazed instead of soldered in order to withstand the additional heat
- (4) replace the switch in one of the heater circuits with a variac. This will give a smooth control of the heat throughout the temperature range.
- (5) replace the glass walls of the test section with pyrex or some other transparent material that will withstand high temperatures and pressures
- (6) secure a suction pump to install at the exit end of the diffuser, so that the vaporization of fuel can be studied at pressures less than the atmospheric pressure which is the pressure range of greater interest

- (7) place a control valve downstream of the test section so that the back pressure can be controlled, thus, controlling the static pressure in the working section.

REFERENCES

- (1) El-Makil, M. M., Uyehara, O. A., and Meyers, P. S., "Theoretical Investigation of the Heating-up Period of Injected Fuel Droplets Vaporizing in Air." National Advisory Committee for Aeronautics, Technical Note 3179. 1954.
- (2) Schubauer, G. B., Spangenberg, W. G., and Klebanoff, P. S., "Aerodynamic Characteristics of Damping Screens." National Advisory Committee for Aeronautics, Technical Note 2001. 1950.
- (3) Dryden, Hugh L., and Schubauer, G. B., "The Use of Damping Screens for the Reduction of Wind-Tunnel Turbulence." Journal of Aeronautical Science, Vol. 14, No. 4. April, 1947. pp. 221-28.
- (4) Robinson, R. F. and Novak, D. H., Introduction to Wind Tunnel Testing (Second Edition). West Lafayette University, University Bookstore. 1952.
- (5) Hilton, W. F., High Speed Aerodynamics. Longmans, Green and Company. 1951.
- (6) Pope, Alan, Wind Tunnel Testing (Second Edition). New York: John Wiley and Sons, Inc. 1954.
- (7) Markowski, S. J., and Moffatt, E. M., "Instrumentation for Development of Aircraft Powerplant Components Involving Fluid Flow." S.A.E. Quarterly Transactions, Vol. 2, 1948. pp. 104-16.
- (8) Eckert, E. R. G., Introduction to the Transfer of Heat and Mass (First Edition). New York: McGraw-Hill Book Company, Inc. 1950.

APPENDIX

LIST OF SYMBOLS

Letters

- A - Surface area, ft^2
- C_p - Specific heat, $\text{btu/lb } ^\circ\text{R}$
- f - Reduction factor
- h - Heat transfer coefficient, $\text{btu/hr ft}^2 ^\circ\text{F}$
- H - Enthalpy, btu/lb
- k - Pressure drop coefficient, dimensionless
- m - Rate of mass flow, lb/sec
- n - Number of screens
- p - Pressure, lb/ft^2
- Q - Quantity of heat, btu
- R - Gas constant, $\text{ft-lb/lb } ^\circ\text{R}$
- t - Temperature, $^\circ\text{F}$
- T - Absolute temperature, $^\circ\text{R}$
- v - Rate of volume flow, ft^3/sec
- V - Velocity, ft/sec

Subscripts

- a - Air-vapor mixture
- b - Baffle
- t - Thermocouple

Greek

ϵ - Emissivity, dimensionless

σ - Constant used in heat transfer ($.1728 \times 10^{-8}$)

ρ - Density, lb/ft³

SAMPLE CALCULATIONS

Example 1

The following is a sample calculation to determine the heater wattage required to raise the temperature of the air flowing through a 20 square inch area test section at 50 feet per second, from 70 F to 250 F, assuming atmospheric pressure.

The rate of mass flow is,

$$m = VA\rho = 50(.139).056 = .389 \text{ lb/sec}$$

where,

$$\rho = \frac{p}{RT} = \frac{14.7(144)}{53.3(710)} = .056 \text{ lb/ft}^3.$$

The Btu's required per pound of air is

$$\begin{aligned} H &= C_p \Delta T \\ &= .24(180) = 43.2 \text{ btu/lb} \end{aligned}$$

where,

$$C_p = .24.$$

Thus, the Btu's required per second is

$$\begin{aligned} mH &= 43.2(.389) \\ &= 16.81 \text{ btu/sec.} \end{aligned}$$

The conversion factor to change btu/sec into watts is 1054.8.

Therefore, the required wattage is equal to 16.81(1054.8), which is 17,750 watts.

The results of the calculations for several test section sizes are shown in graph form in Figure 7.

Example 2

This sample calculation is to show the method used in determining the displacement required for a four-cycle engine operating at 2000 rpm to produce a flow of 50 feet per second in a test section with a cross-sectional area of 20 square inches.

The volume flow (v) through the tunnel is

$$\begin{aligned} v &= VA \\ &= 50(.139) = 6.95 \text{ ft}^3/\text{sec.} \end{aligned}$$

The number of displacements per second for the 2000 rpm, 4-cycle engine is 16.67, since it takes two revolutions for one complete displacement. Therefore, the required displacement is,

$$= \frac{6.95(1728)}{16.67} = 720 \text{ cubic inches.}$$

The results of the calculations for several test section sizes are shown in graph form in Figure 14.

Example 3

A sample calculation to obtain the possible error that can be expected in the temperatures recorded by the wet-mixture thermocouple probes follows:

At equilibrium,

$$Q_{in} = Q_{out}$$

and,

$$h(T_a - T_t) = \sigma \epsilon (T_t^4 - T_b^4)$$

for,

$$\frac{Q_{in}}{A} = h(T_a - T_t) \text{ and } \frac{Q_{out}}{A} = \sigma \epsilon (T_t^4 - T_b^4).$$

The following values are assumed to simulate a practical problem.

$$T_a = 620^{\circ}\text{R}$$

$$T_b = 520^{\circ}\text{R}$$

$$\epsilon = 0.9$$

$$h = 10 \text{ btu/hr ft}^2 \text{ }^{\circ}\text{F.}$$

The value of 0.9 for ϵ was assumed since welded thermocouples are fairly good radiators of heat.

The value, $h = 10$, was assumed since the sensing element of the thermocouple probe is located in the wake of a 60 degree right circular cone baffle. According to Eckert (Reference 8), the range for h is 2 to 50 for flowing air, where 2 is a normal value in slowly moving air and 50 is a normal value in rapidly moving air.

With the above assumed values,

$$\frac{Q_{in}}{A} = 10(620 - T_t) \text{ and}$$

$$\frac{Q_{out}}{A} = .173(.9) \left[\left(\frac{T_t}{100} \right)^4 - \left(\frac{500}{100} \right)^4 \right] .$$

The following values for $\frac{Q_{in}}{A}$ and $\frac{Q_{out}}{A}$ were obtained by assuming three values for T_t .

T_t	$\frac{Q_{in}}{A}$	$\frac{Q_{out}}{A}$
610	100	102.0
600	200	88.2
590	300	75.0

A graph using the above values was plotted with $\frac{Q}{A}$ as the ordinate and T as the abscissa and is shown in Figure 34.

From the graph it can be seen that the point where $Q_{in} = Q_{out}$ the temperature is approximately 150 F. Since the temperature assumed for the air was 160 F, the thermocouple reading would be in error by 10 degrees or 6.27 per cent.

Example 4

A sample calculation showing the calculations necessary to convert the dynamic pressure of the flow in the test section, measured in inches of alcohol, into the velocity of the air stream follows:

Measured values:

Dynamic pressure = 2.45 inches of alcohol

Barometric pressure = 32.00 inches of Hg.

Temperature of the air = 670°R

Therefore, since $p = (.491)32.00 = 15.7$ psia and

$$p = \rho RT$$

$$\rho = \frac{15.7(144)}{670(1715)}$$

$$= .00197 \text{ slugs/ft}^3.$$

Dynamic pressure ($1/2 \rho V^2$) is equal to the total pressure minus the static pressure and was measured on the manometer board to be 2.45 inches of alcohol. The specific gravity of the alcohol is .806, therefore, 2.45 inches of alcohol is equal to 1.975 inches of water.

$$p = 1.975(5.204)$$

$$= 10.28 \text{ lb/ft}^2$$

$$p = 1/2 \rho V^2$$

$$V^2 = \frac{2(10.28)}{.00197}$$

$$V = 102 \text{ ft/sec.}$$

Table I. Velocity Profile Data

Station 10

Distance From Top (Inches)	Inches of Alcohol	Dynamic Pressure (#/Ft ²)	$V = \frac{2P}{\rho}$ (Ft ² /Sec ²)	V (Ft/Sec)
Left Tap Looking Upstream				
.25	2.40	10.01	10,200	101.0
.75	2.40	10.01	10,200	101.0
1.75	2.45	10.27	10,390	101.8
2.75	2.45	10.27	10,390	101.8
3.25	2.45	10.27	10,390	101.8
3.90	1.70	7.13	7,210	84.9
Right Tap Looking Upstream				
.25	2.30	9.64	9,760	98.7
.75	2.40	10.01	10,200	101.0
1.75	2.40	10.01	10,200	101.0
2.75	2.45	10.27	10,390	101.8
3.25	2.45	10.27	10,390	101.8
3.90	2.00	8.38	8,490	91.5
Center Line Tap				
.25	2.10	8.81	8,920	94.5
.75	2.40	10.01	10,200	101.0
1.75	1.95	8.17	8,270	90.3
2.75	2.35	9.85	9,980	99.2
3.25	2.40	10.01	10,200	101.0
3.90	1.30	5.45	5,520	74.3

Table II. Velocity Profile Data

Station 18				
Distance From Top (Inches)	Inches of Alcohol	Dynamic Pressure (#/Ft ²)	$v^2 = \frac{2P}{\rho}$ (Ft ² /Sec ²)	V (Ft/Sec)
Left Tap Looking Upstream				
.25	1.80	7.45	7,600	87.1
.75	2.45	10.27	10,390	101.8
1.75	2.45	10.27	10,390	101.8
2.75	2.50	10.48	10,600	102.9
3.75	1.95	8.17	8,270	90.9
3.95	1.05	4.40	4,450	66.6
Right Tap Looking Upstream				
.25	1.75	7.33	7,420	86.1
.75	2.40	10.01	10,200	101.0
1.75	2.40	10.01	10,200	101.0
2.75	2.40	10.01	10,200	101.0
3.75	2.00	8.38	8,480	92.0
3.95	1.50	6.28	6,350	79.6
Center Line Tap				
.25	1.90	7.96	8,050	89.7
.75	2.45	10.27	10,390	101.8
1.75	2.10	8.80	8,910	93.8
2.75	2.40	10.01	10,200	101.0
3.75	1.80	7.54	7,620	87.3
3.95	1.15	4.82	4,880	69.9

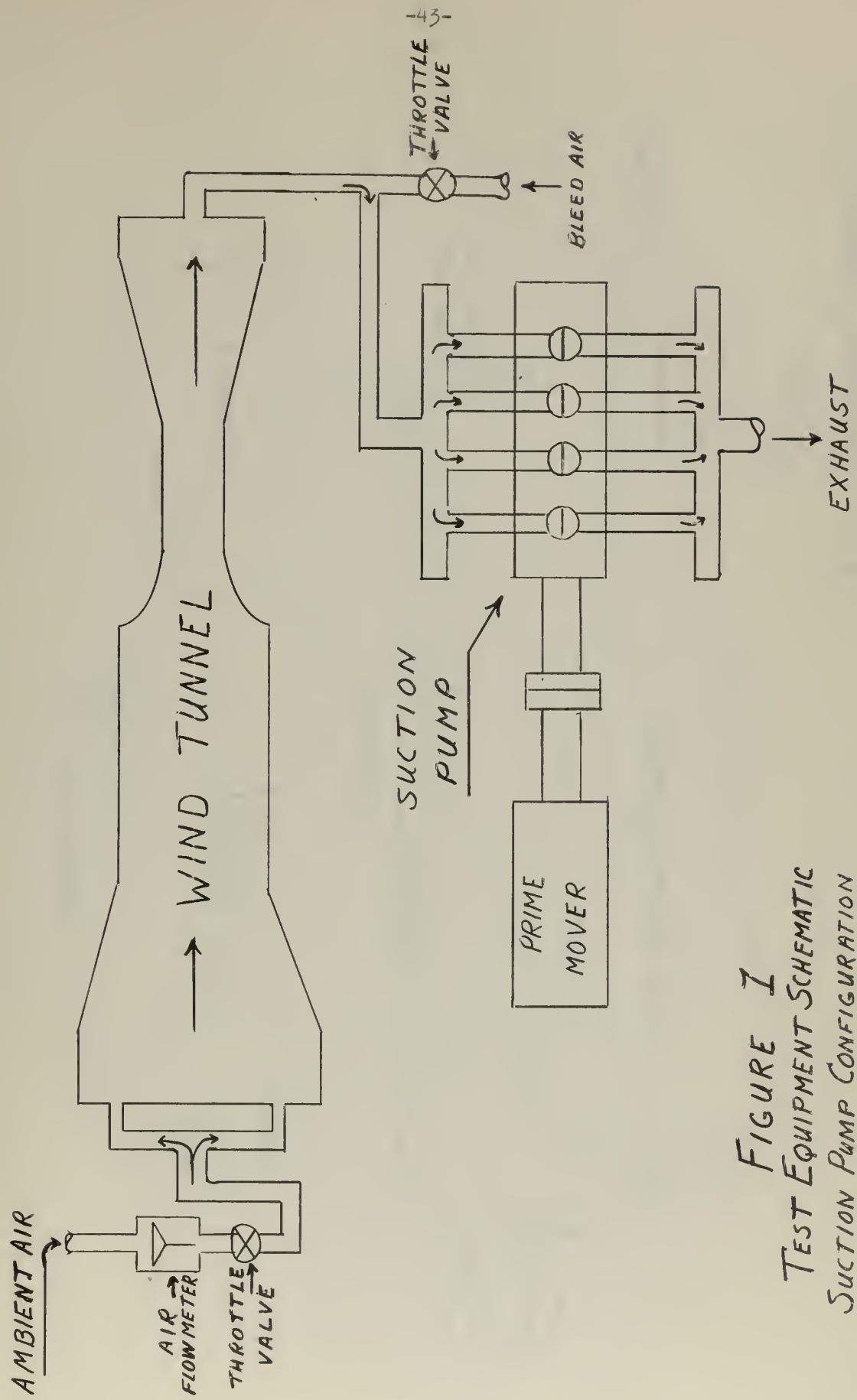


FIGURE I
TEST EQUIPMENT SCHEMATIC
SUCTION PUMP CONFIGURATION

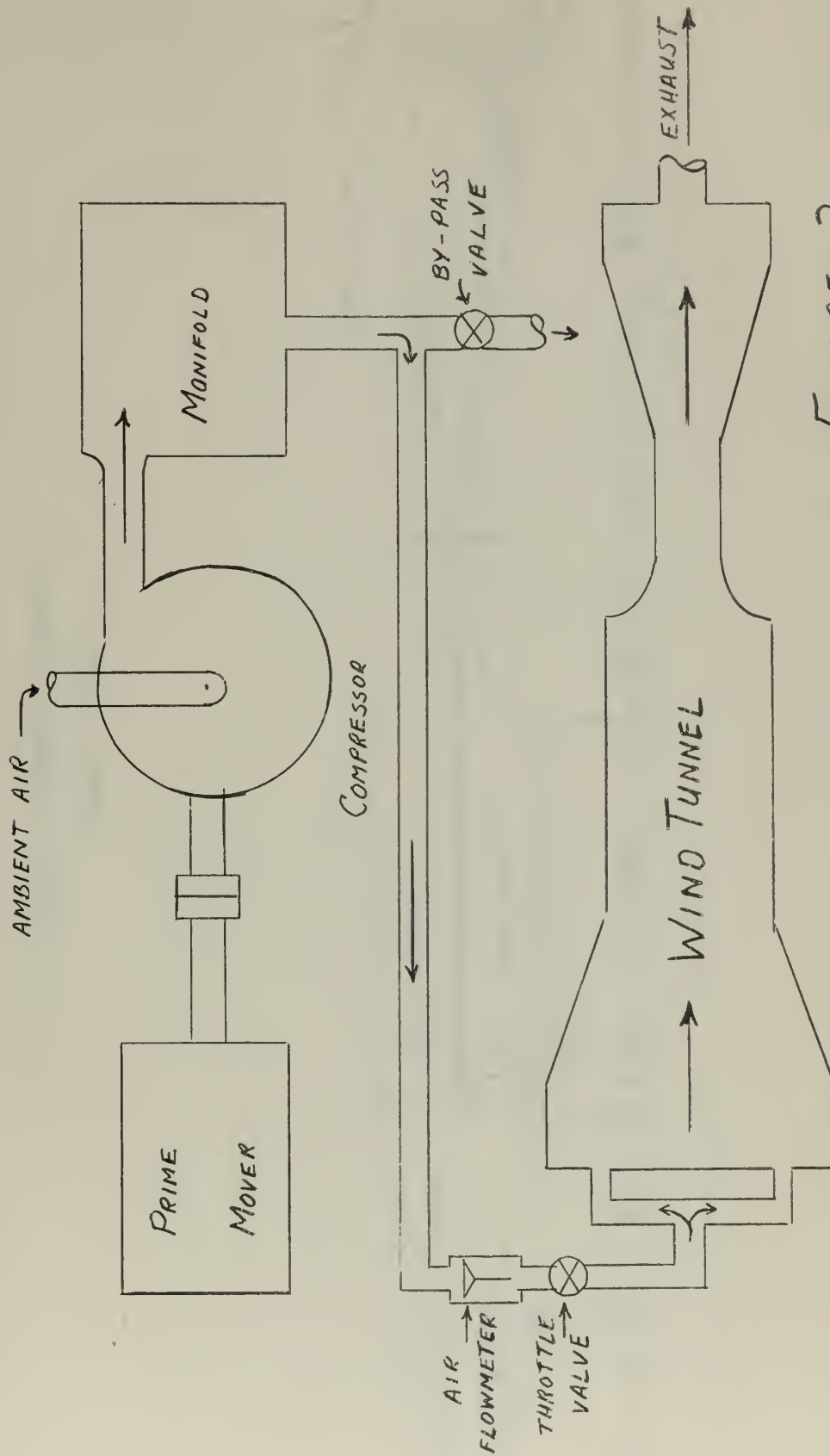
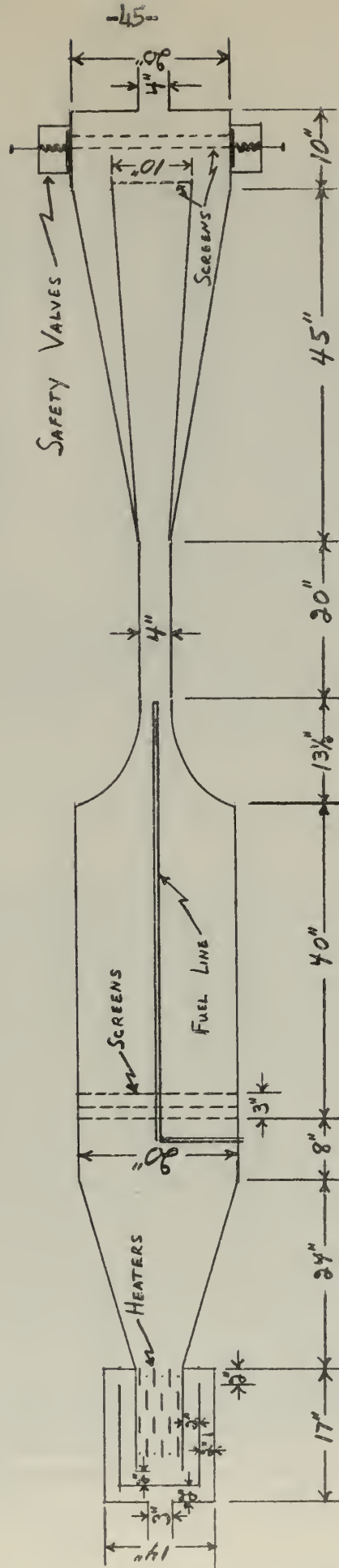


FIGURE 2
TEST EQUIPMENT SCHEMATIC
COMPRESSOR CONFIGURATION

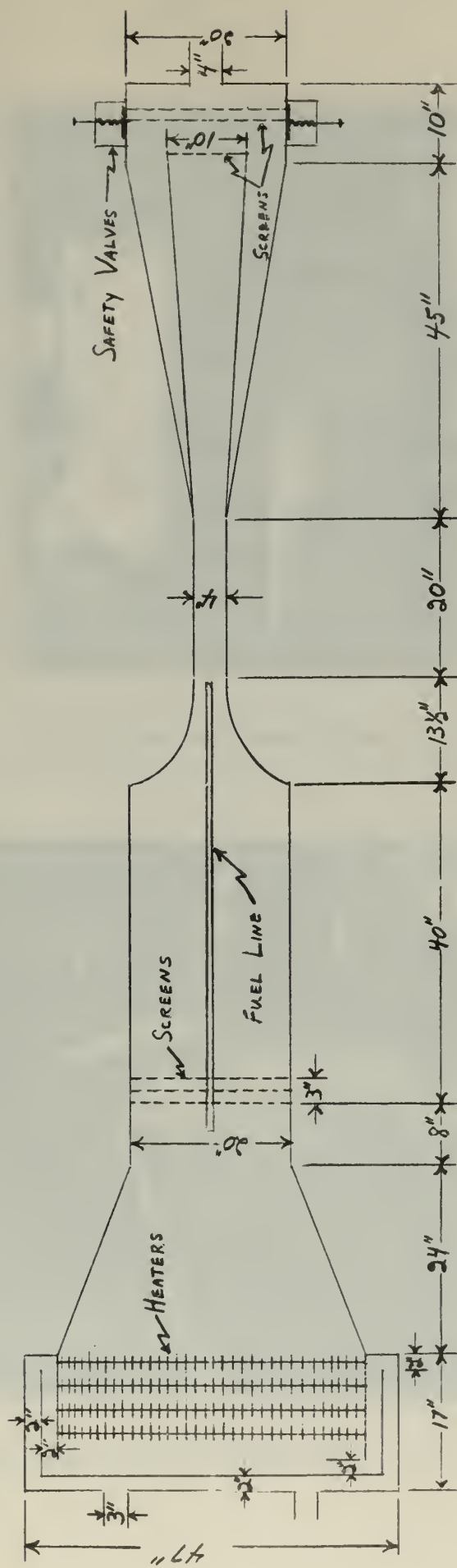
WIND TUNNEL SKETCH
SIDE VIEW



3
F. 6.

SCALE 1:20

WIND TUNNEL SKETCH Top View



SCALE 1:20

FIG. 4

Wind Tunnel

Fuel

Fuel Spray

Vaporization

Design



Fig. 5 Wind Tunnel and Accessories



Fig. 6 Heater Section Assembled



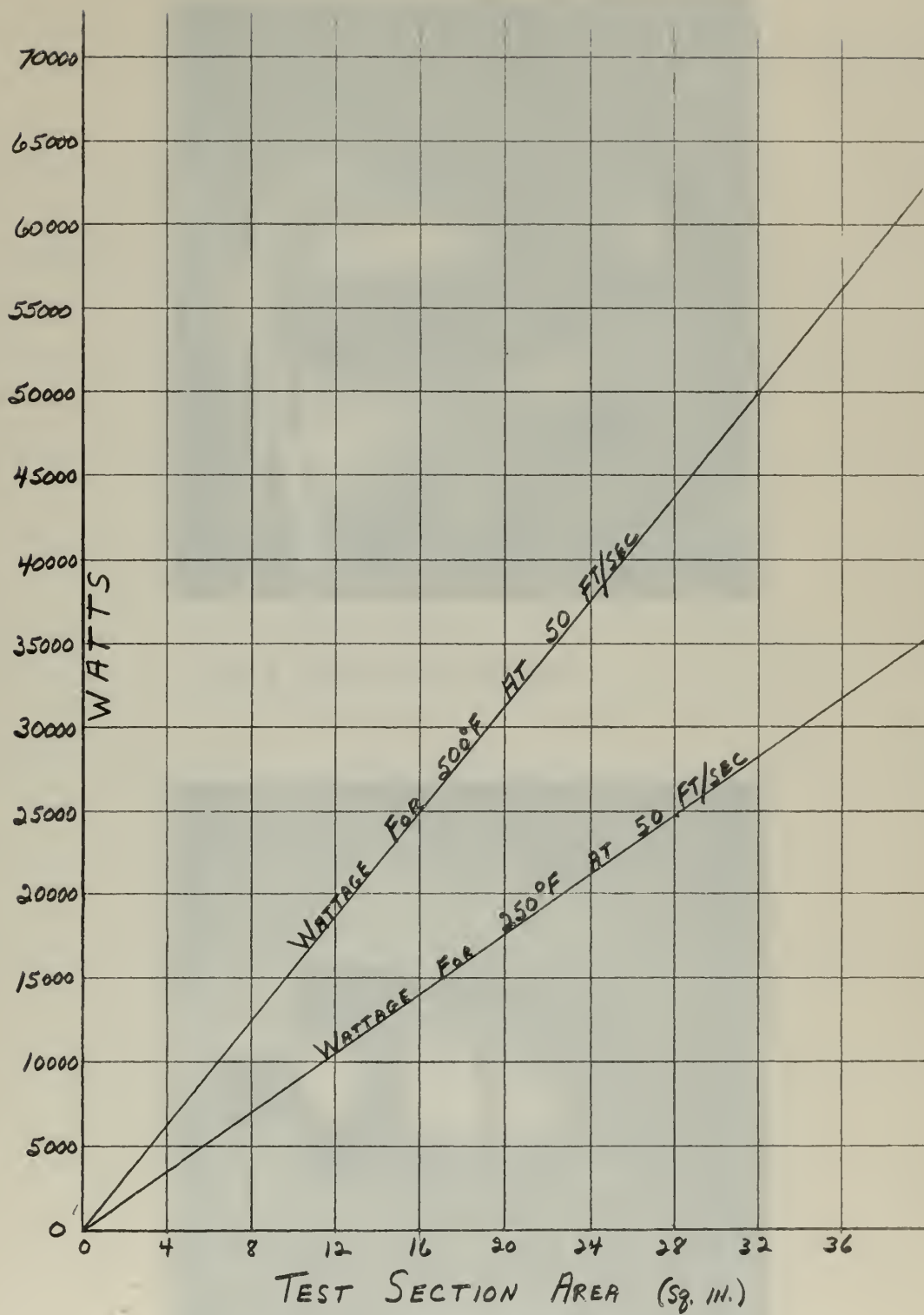


FIG. 7

1 2 3 4 5 6 7 8 9 10 11 12 13 14 15 16 17 18 19 20 21 22 23 24 25 26 27 28 29 30 31 32 33 34 35 36 37 38 39 40 41 42 43 44 45 46 47 48 49 50 51 52 53 54 55 56 57 58 59 60 61 62 63 64 65 66 67 68 69 70 71 72 73 74 75 76 77 78 79 80 81 82 83 84 85 86 87 88 89 90 91 92 93 94 95 96 97 98 99 100





Fig. 8 Heater Installation



Fig. 9 Settling Chamber and Contraction
Nozzle



HEATER ELECTRICAL CIRCUIT

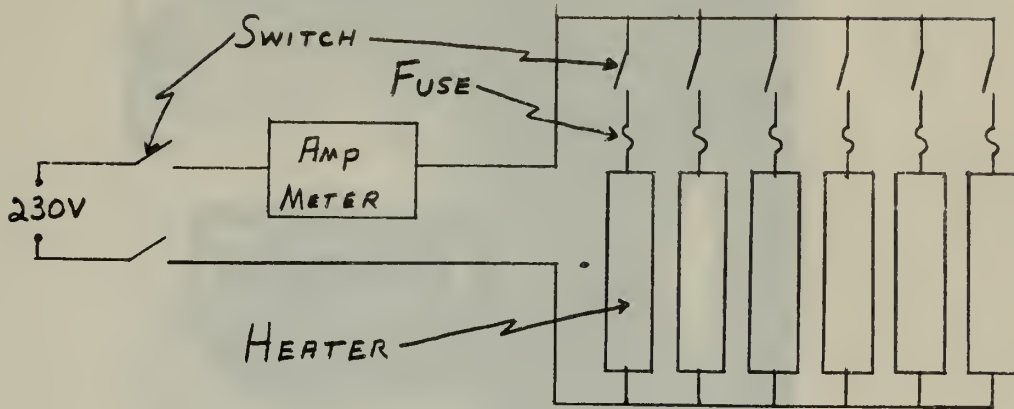


FIG. 10

THERMOCOUPLE CIRCUIT

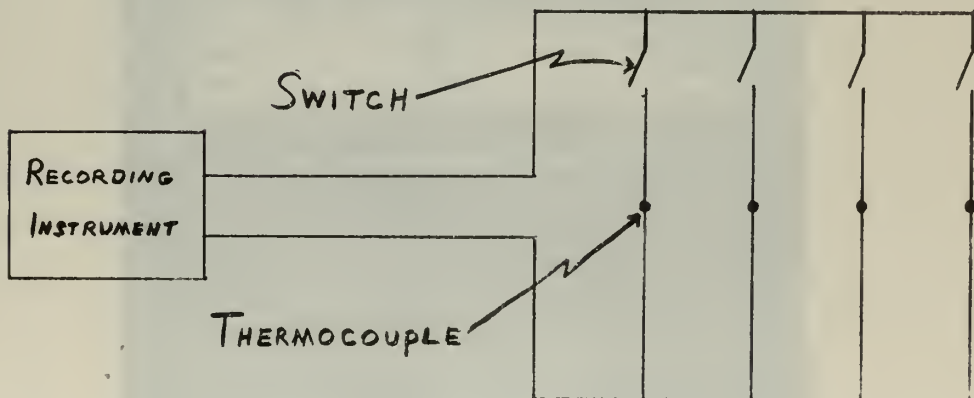


FIG. 11

THE HISTORY OF THE



PLATE I

THE HISTORY OF THE

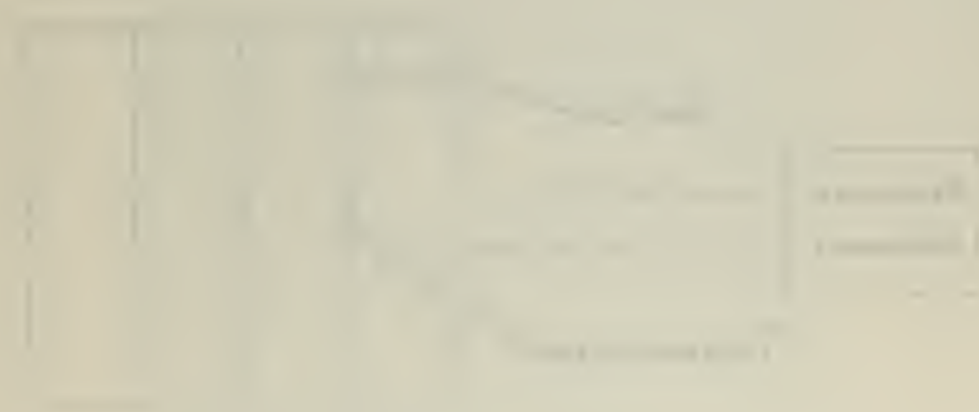


PLATE II



Fig. 12 Test Section

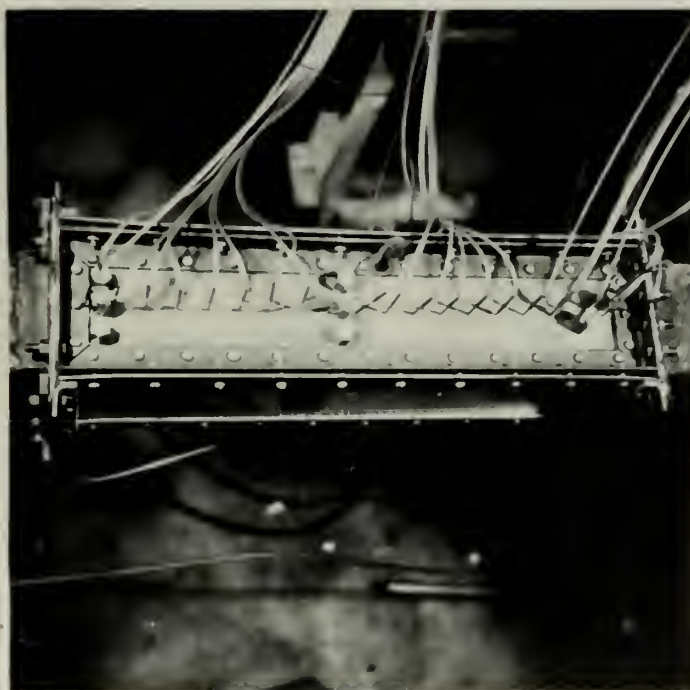


Fig. 13 Test Section To View



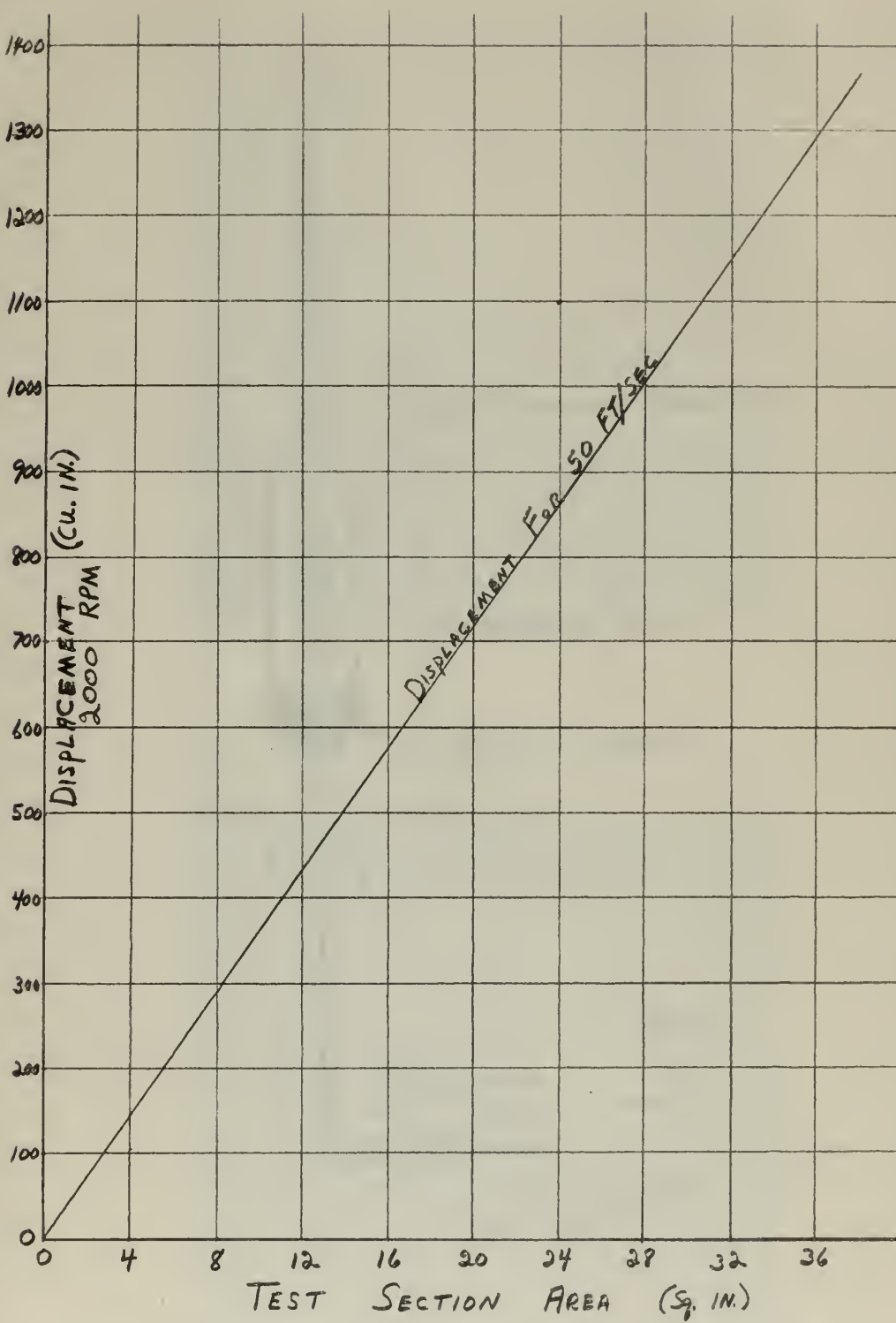
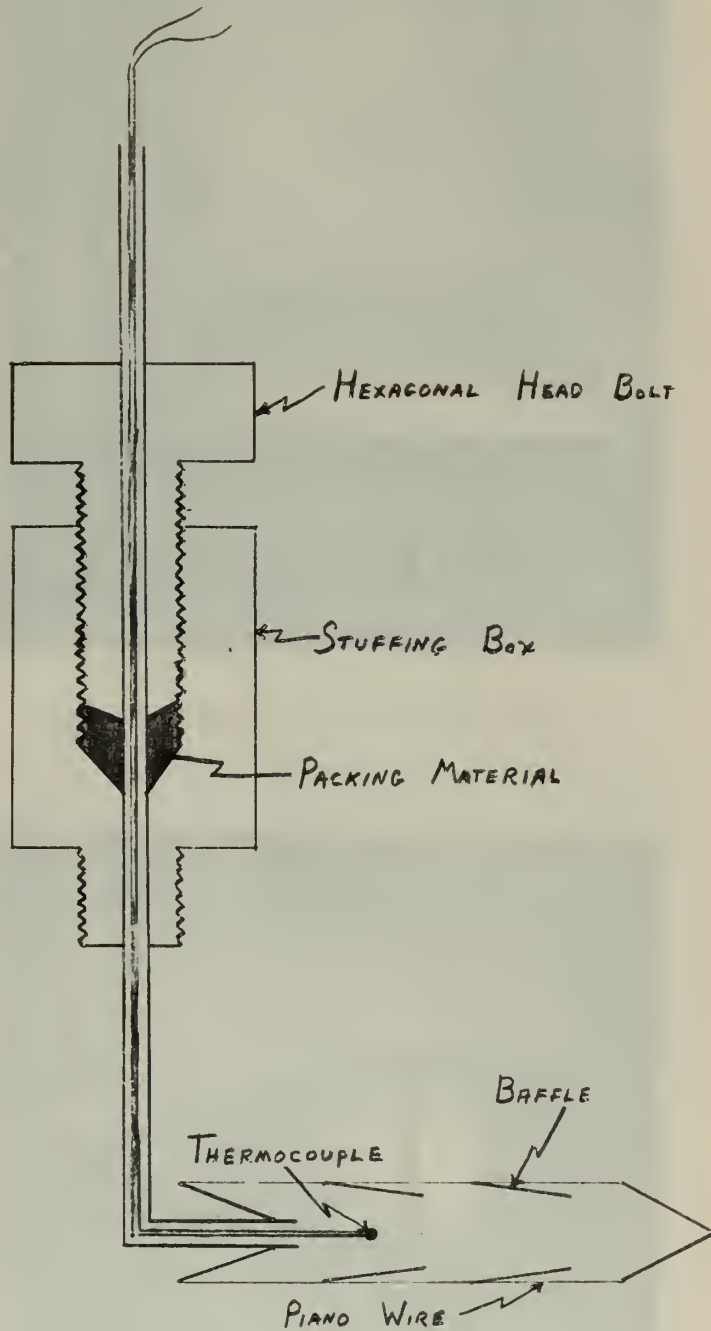


FIG. 14





WET-MIXTURE THERMOCOUPLE AND STUFFING BOX

FIG. 15

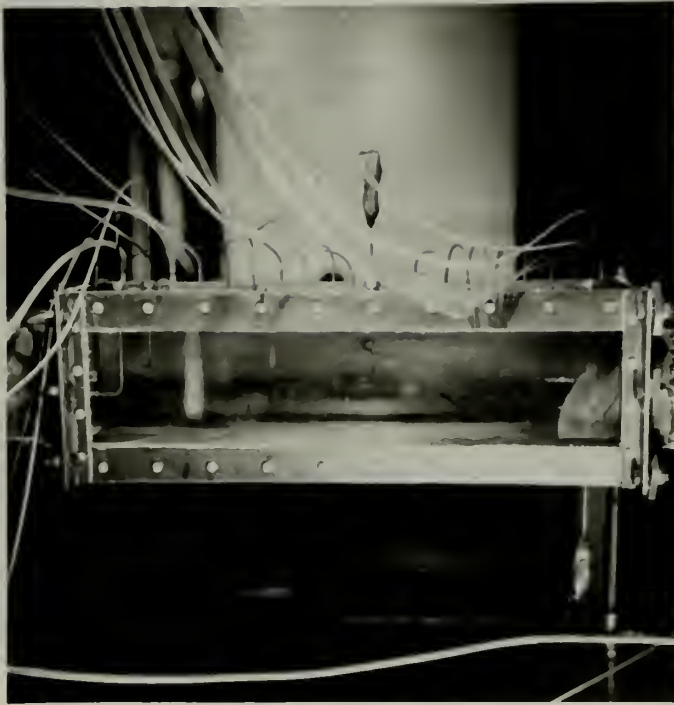


Fig. 16 Test Section Side View



Fig. 17 Diffuser and Surge Tank



Fig.18 Suction Pump Side View

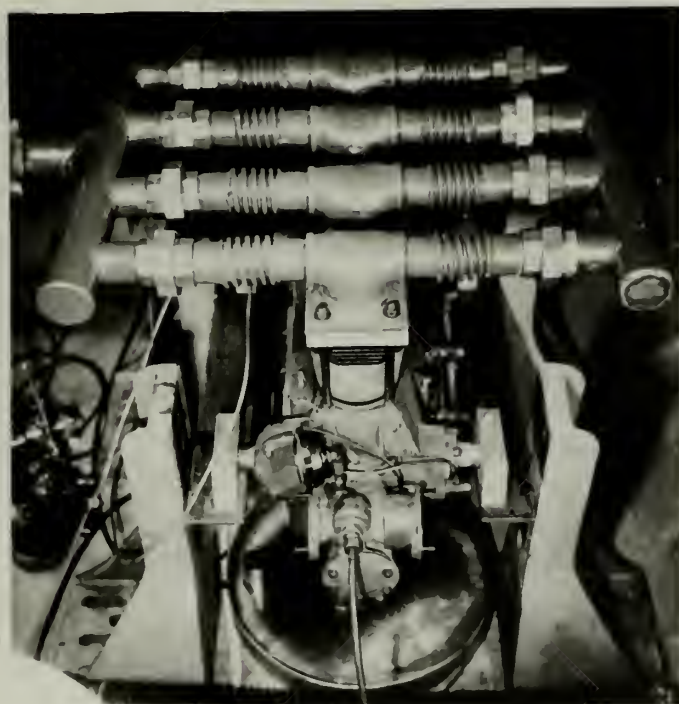


Fig.19 Suction Pump Top View



Fig. 20 Engine and Compressor



Fig. 21 Control Panel for Engine Operation

FUEL SYSTEM

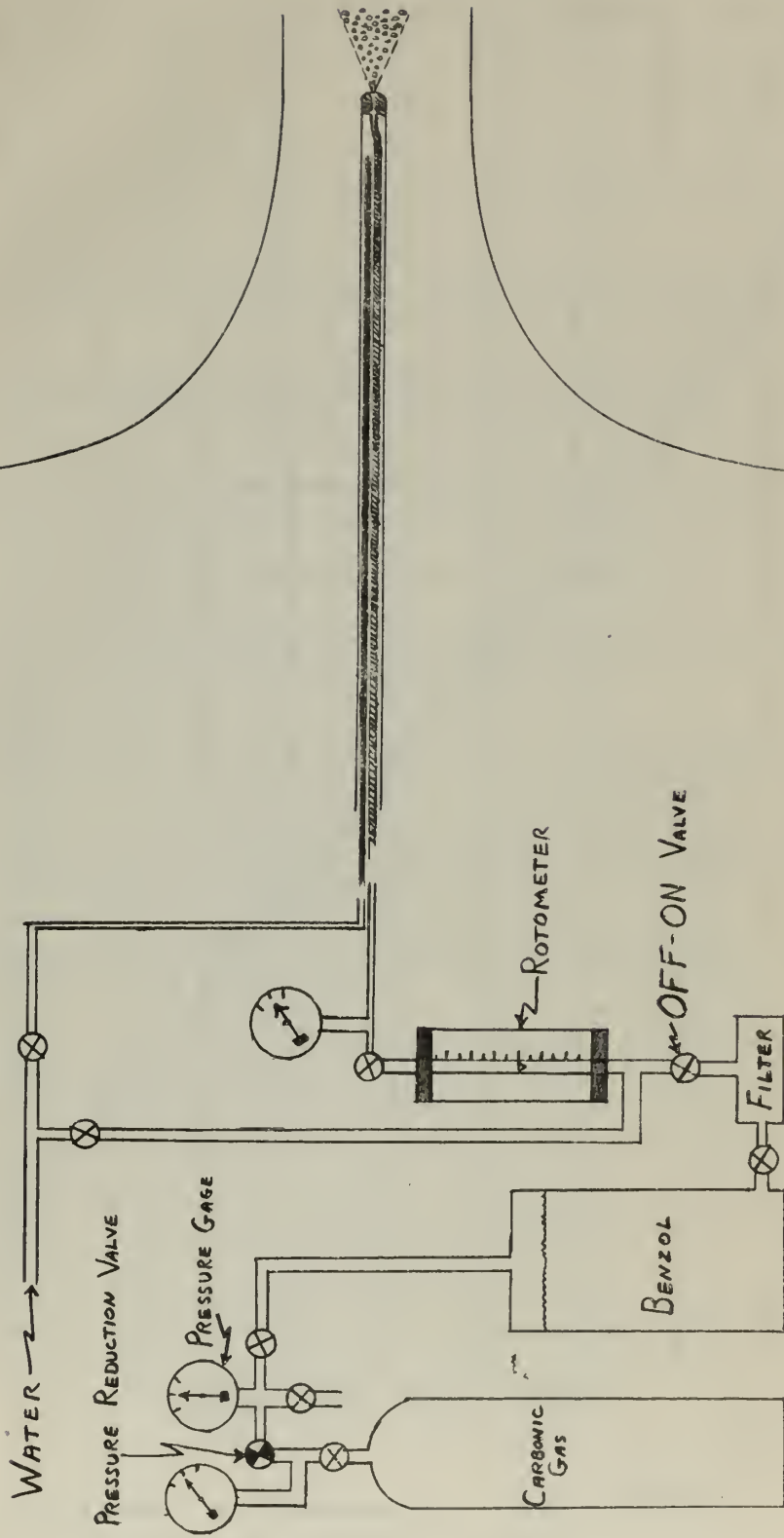
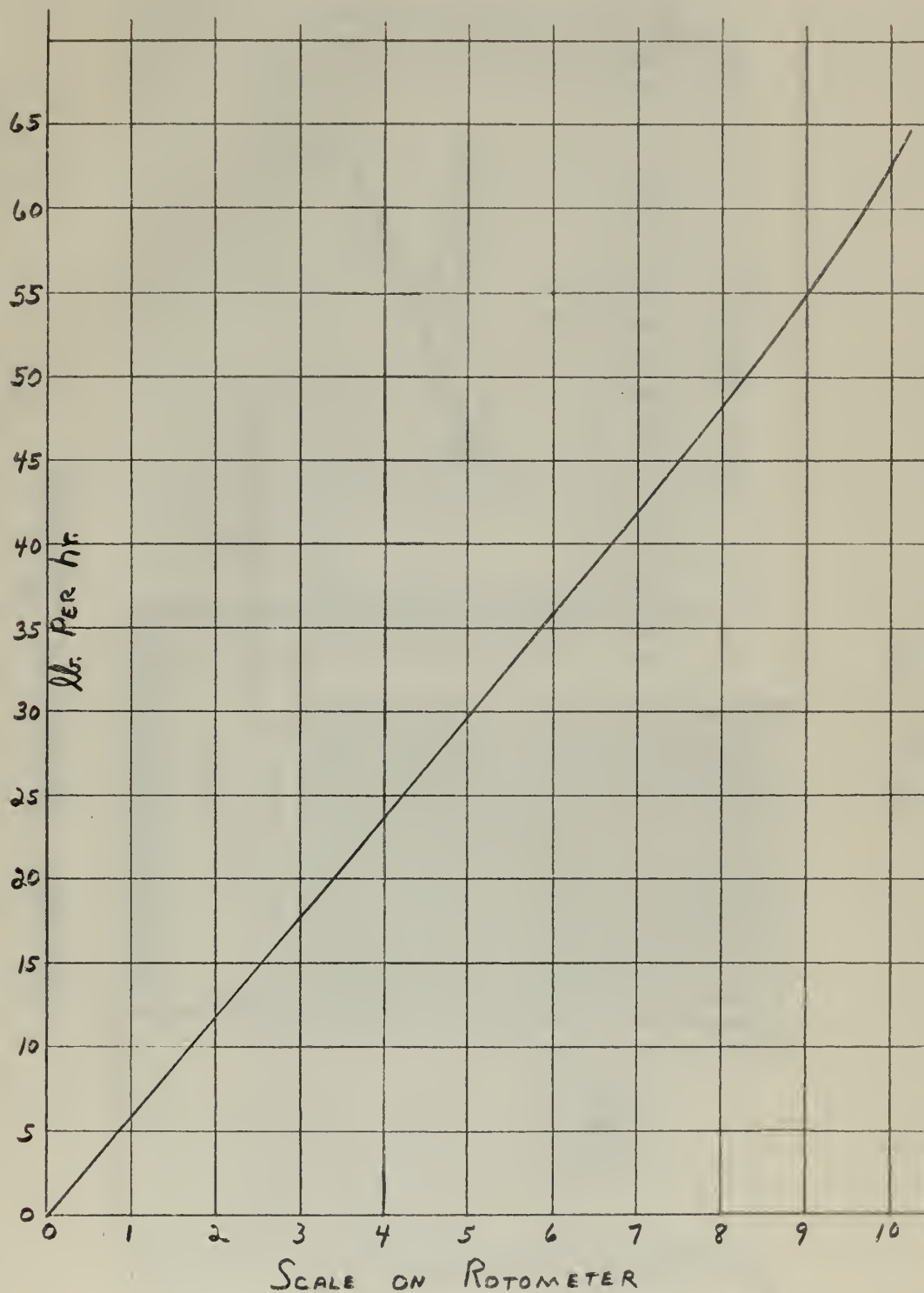


FIG. 22



CALIBRATION OF ROTOMETER FOR BENZOL
SPECIFIC GRAVITY 0.8704

FIG. 23

PRESSURE MEASURING SYSTEM

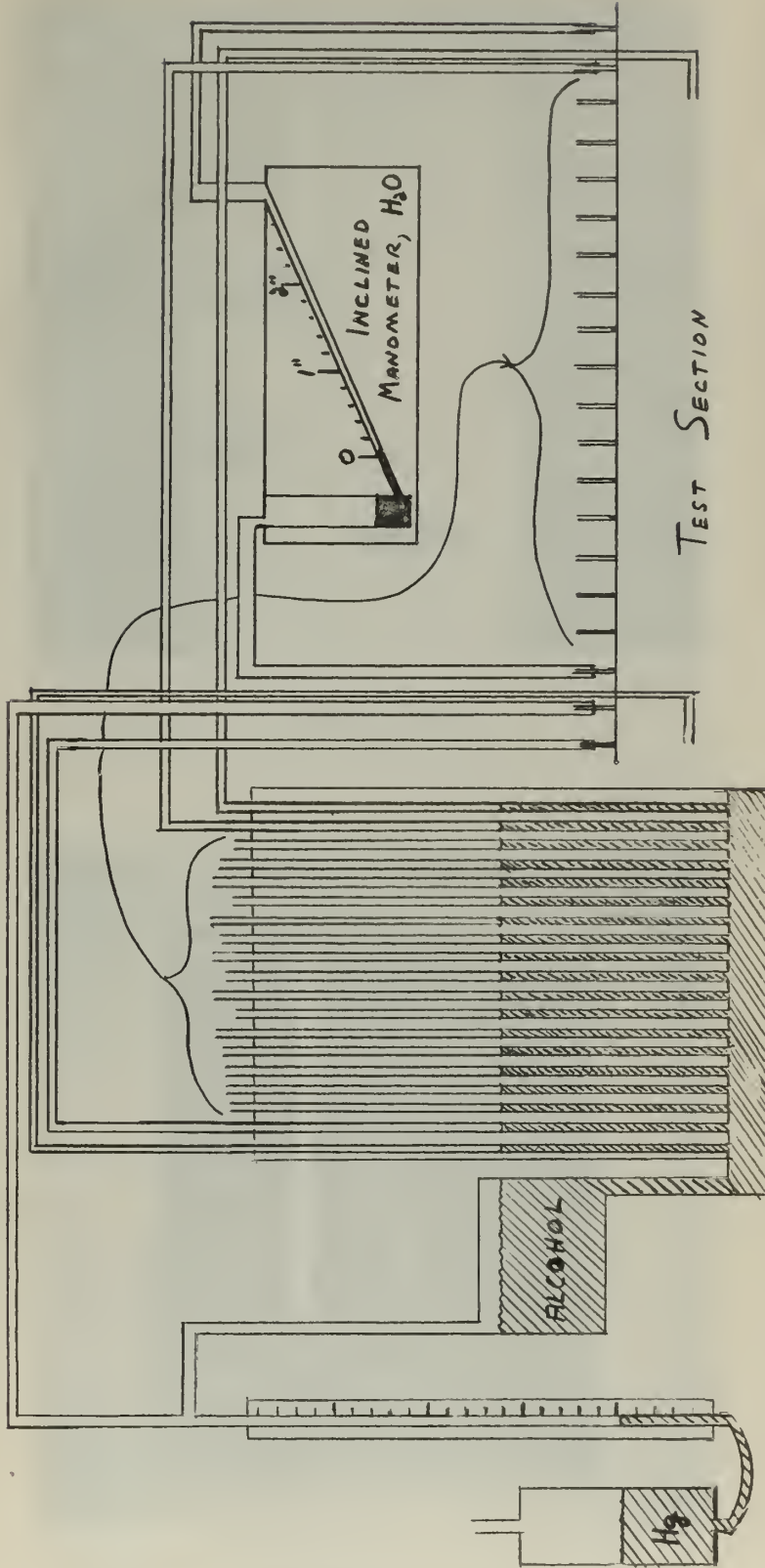


FIG. 24



Fig. 25 Instrument Panel



Fig. 26 Thermocouple Probe

DIAGRAM OF SMOKE PROBE TEST FOR ONE DIMENSIONAL FLOW

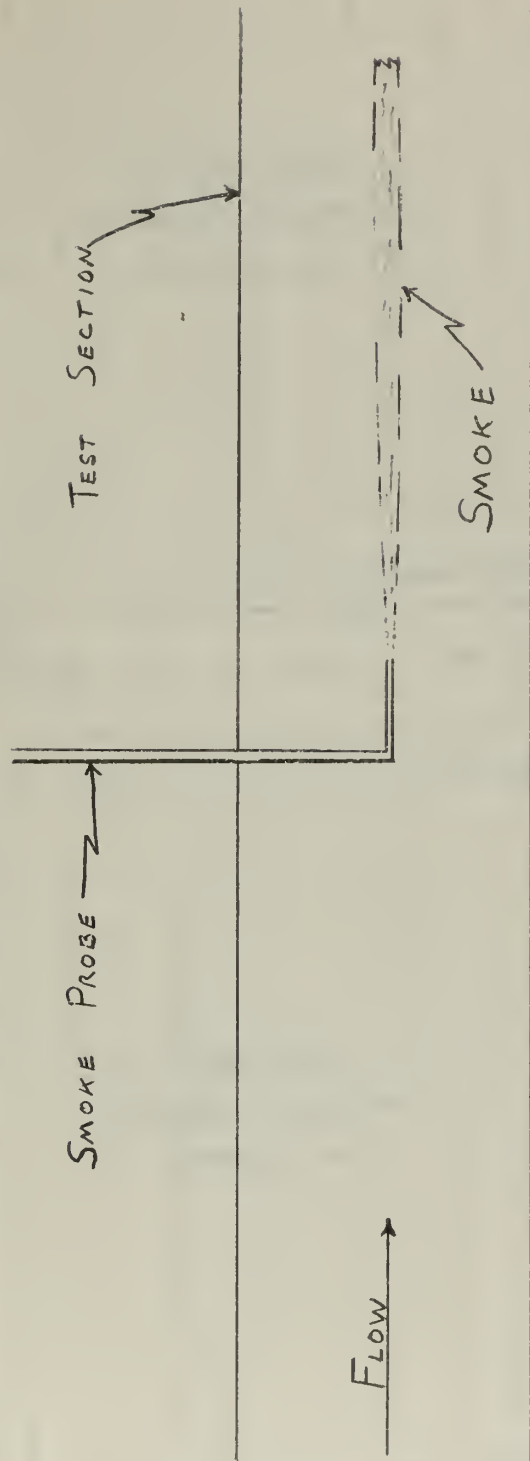


FIG. 27

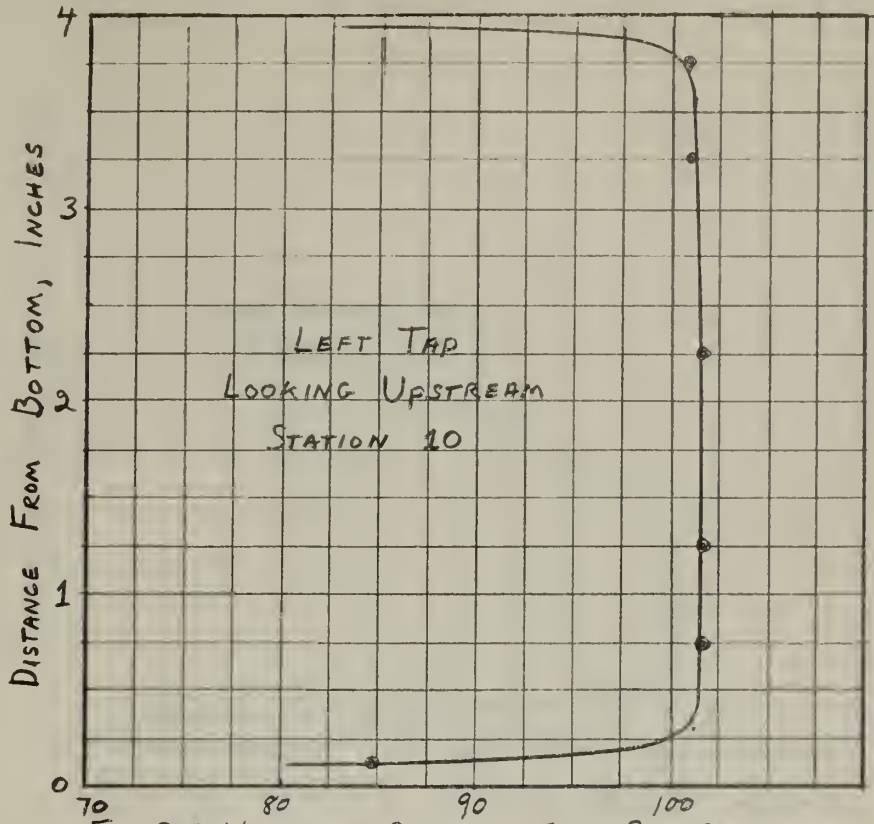


FIG. 28. VELOCITY PROFILE, FEET PER SECOND.

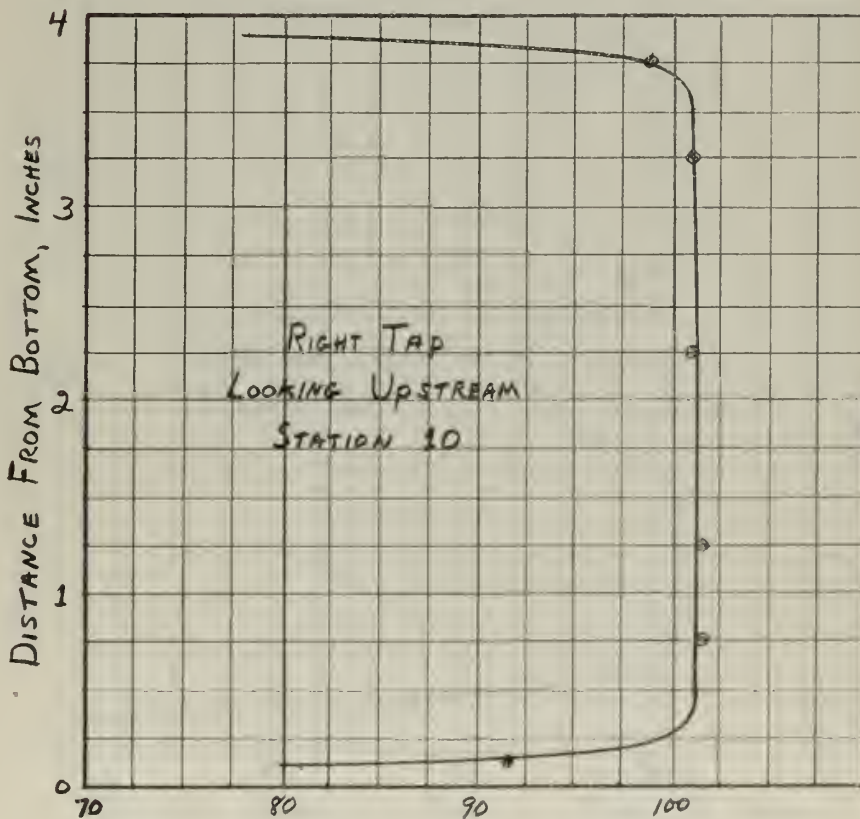
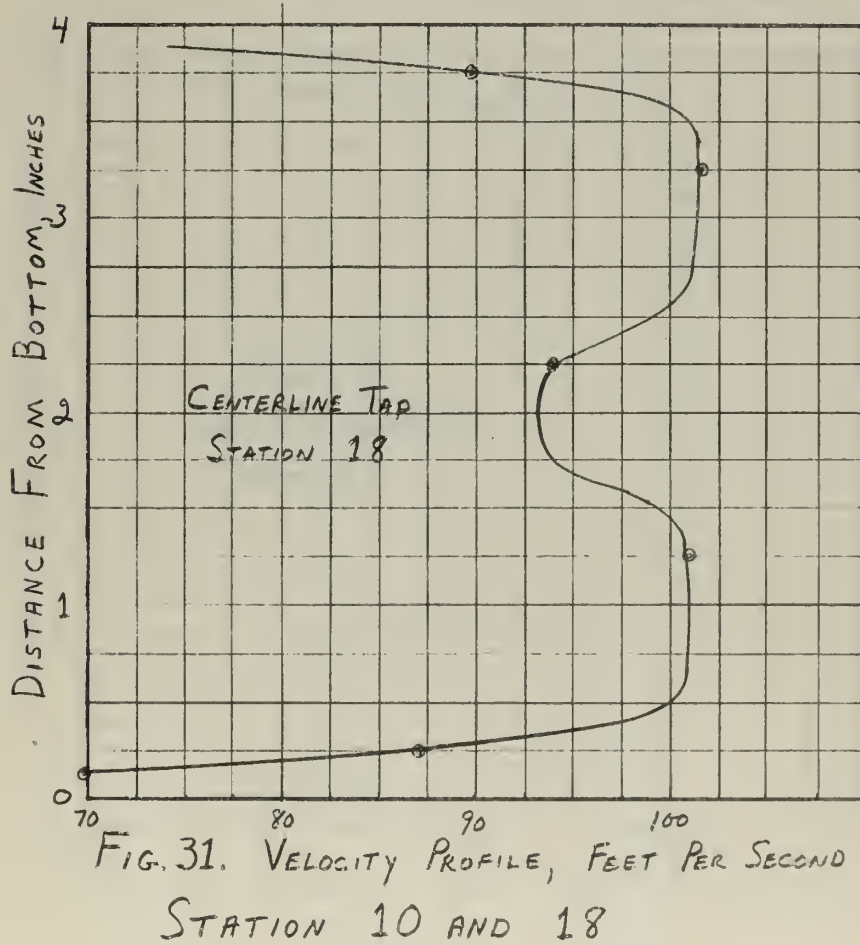
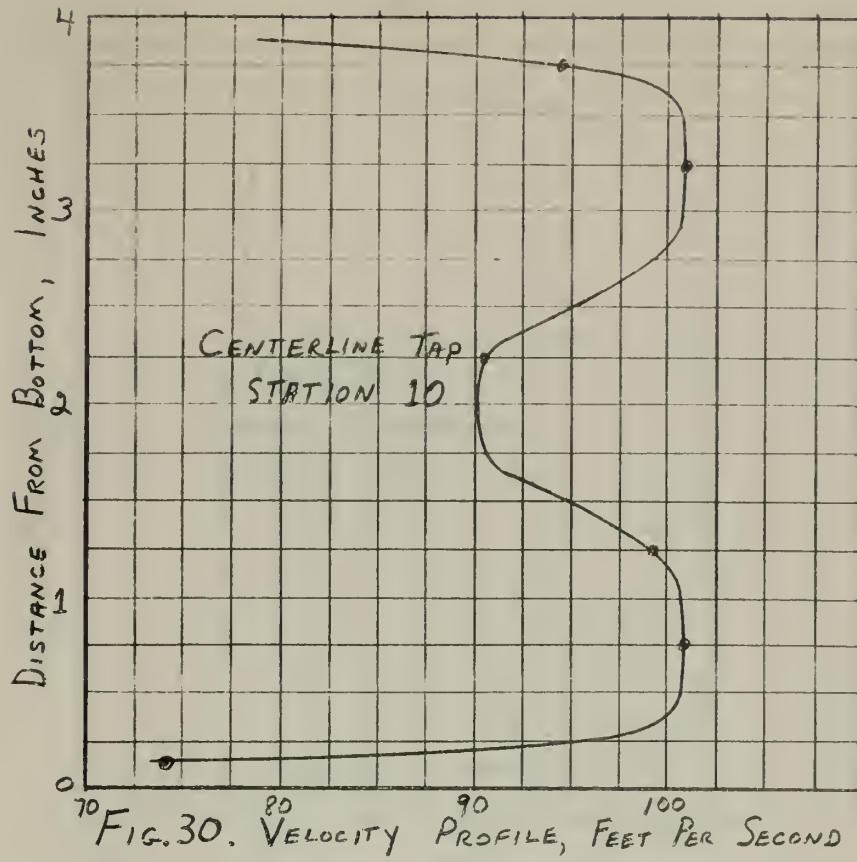
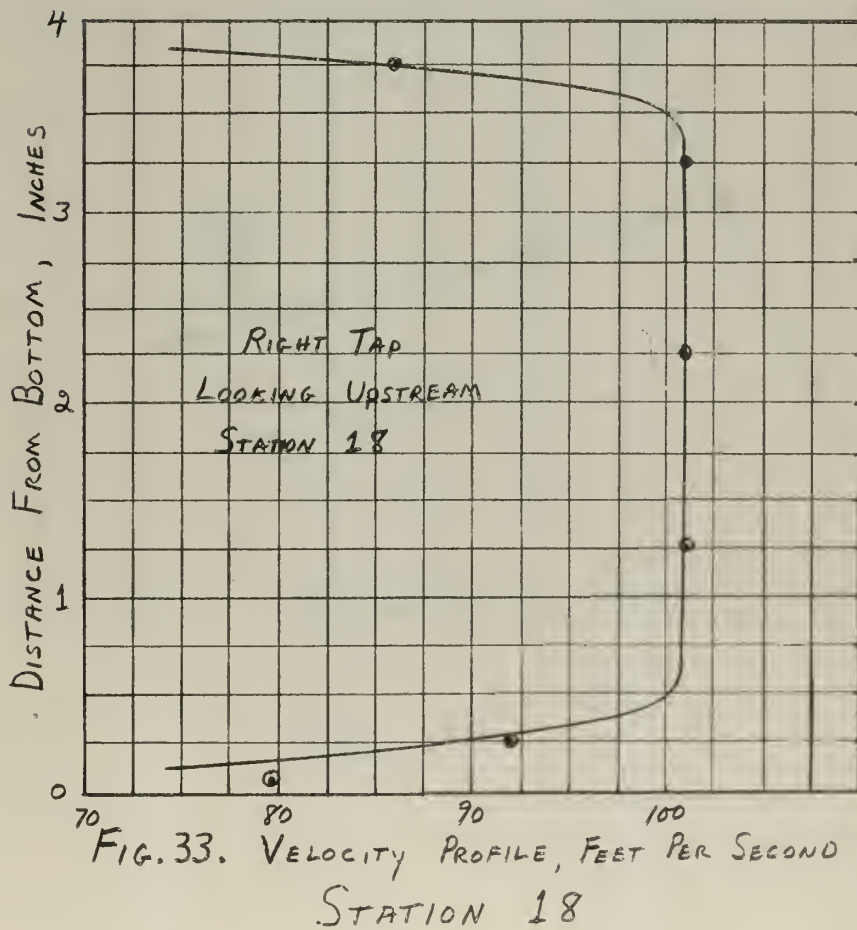
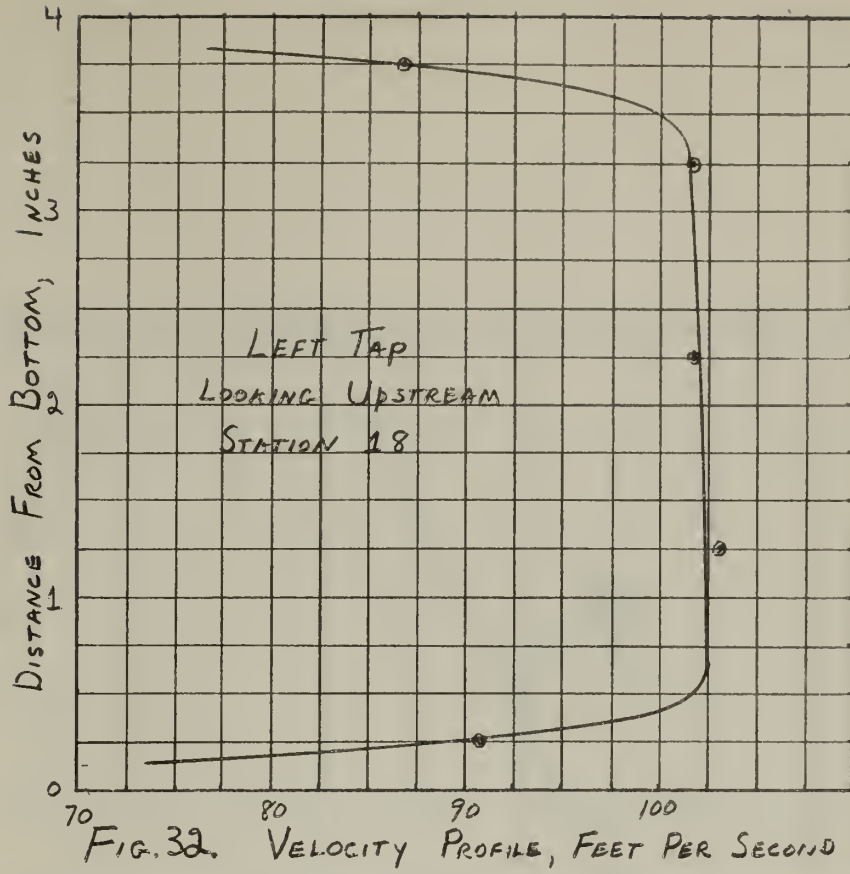


FIG. 29. VELOCITY PROFILE, FEET PER SECOND.

STATION 10





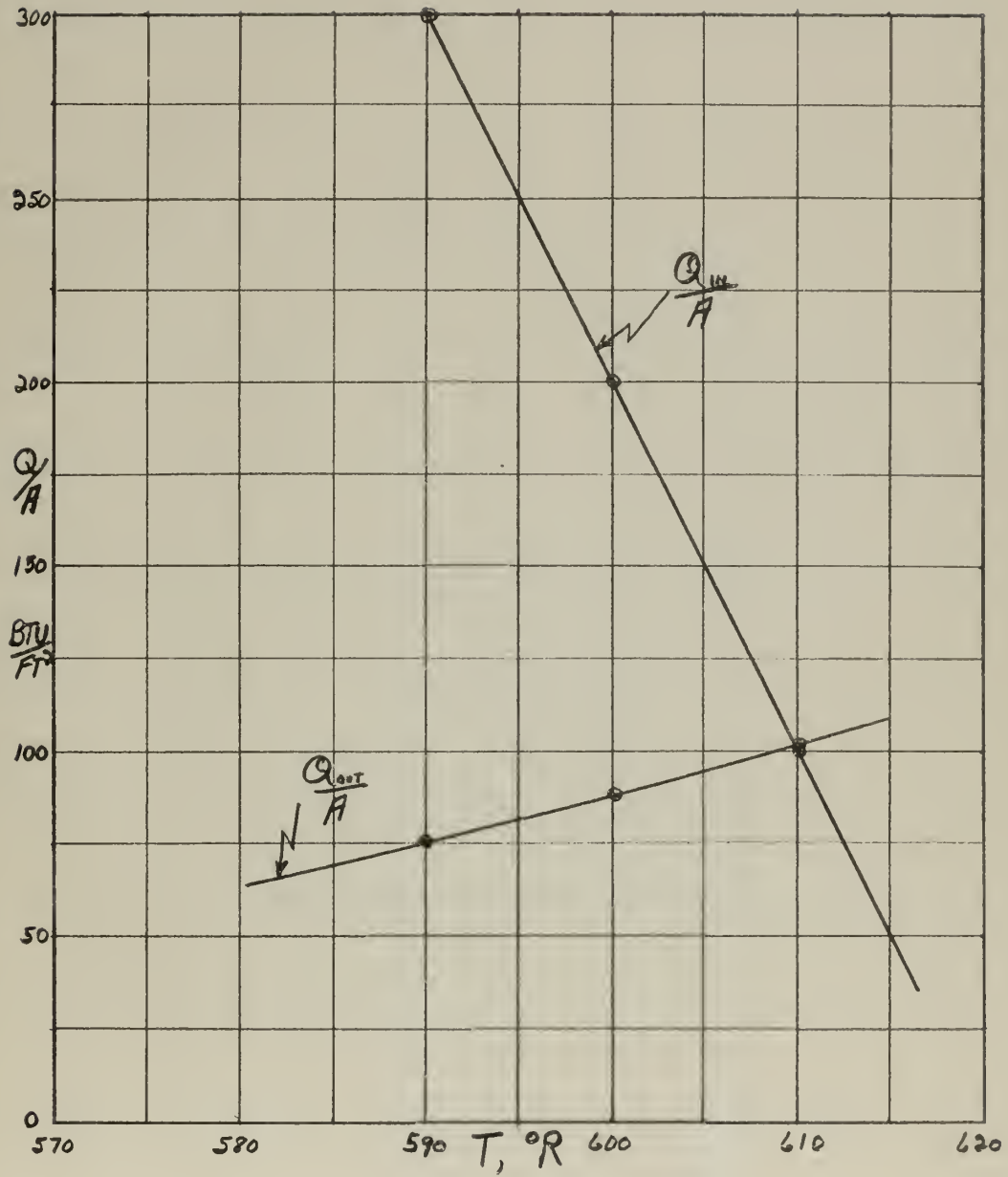


FIG. 34

Thesis
F229

Farnsworth

33158

The design of a wind
tunnel for fuel spray
vaporization studies.

Thesis
F229

Farnsworth

33158

The design of a wind tunnel
for fuel spray vaporization
studies.

thesF229

The design of a wind tunnel for fuel spr



3 2768 002 13379 5

DUDLEY KNOX LIBRARY